Practical Viability of Naturally-Occurring Ilmenite as a Catalyst in Advanced Oxidation Processes

By

Alicia Levana Butt

Submitted in partial fulfilment of the requirements for the degree

Masters of Applied Science

In

Environmental Technology

In the Faculty of Engineering, Built Environment and Information Technology

Department of Chemical Engineering

University of Pretoria

September 2021

ABSTRACT

Title:	Practical Viability of Naturally-Occurring Ilmenite as a Catalyst in AOPs
Author:	Alicia Levana Butt
Supervisor:	Dr Shepherd M Tichapondwa
Institution:	University of Pretoria
Faculty:	Engineering, Built Environment and Information Technology
Department:	Chemical Engineering
Division:	Water utilisation and Environmental Engineering
Degree:	Masters of Science (Applied Science) Environmental Technology

The demand for clean, quality, portable water is ever-increasing due to the global demand. One way to address this demand is through water reuse. Water becomes contaminated through many anthropogenic processes, and thus newer technologies are required to purify the water to acceptable standards. One of the main issues in wastewater is the presence of highly stable organic compounds that are resistant to conventional wastewater treatment. Advanced Oxidation Processes (AOPs) are relatively successful at degrading such compounds. One of the most commonly used AOP is the Fenton's reagent, which uses iron salts and hydrogen peroxide to generate highly oxidising free radicals. However, this method has limitations as it tends to generate secondary waste streams with high iron concentrations.

This work aims to investigate naturally occurring ilmenite ($FeTiO_3$) as a viable catalyst for Fenton-like reactions to combat the limitations of the original reaction. Methyl Orange (MO) was chosen as a model compound in this study due to its high stability and resistance to conventional degradation methods. The catalyst was characterised by X-ray Diffraction (XRD), X-ray Fluorescence (XRF), Scanning Electron Microscopy (SEM/SEM-EDS) and Brunauer-Emmett-Teller (BET) surface area. The catalyst contained ilmenite predominately at

83.53 %, Hematite (Fe_2O_3) at 14.99 % and rutile at 1.2 %. These results are further supported by the SEM-EDS and XRF results.

Degradation studies were carried out in the absence and presence of irradiation in a batch reactor. Under initial operating conditions, complete decolourisation was observed following 90 min of reaction time. The catalyst was recovered following 24 hours of reaction time and reanalysed in terms of XRD. The recovered material had similar XRD spectra as the original catalyst. This indicates that the material can be regarded as a catalyst.

The process was optimised for pH, irradiation, catalyst loading and H_2O_2 dosage. An optimal pH of 2.5 under the presence of UVB irradiation led to the fastest rate of degradation. Iron leaching tests were done simultaneously with the pH optimisation. It was observed that at a pH of 5.0, no degradation or iron leaching occurred. This indicated that iron in solution was necessary for the reaction to occur. Thus, the reaction behaves more like a homogeneous system than a heterogenous system. Although iron leaching does occur, the XRD make-up of the catalyst did not change. Iron leaching was found to reach levels of 1.0 mg/L at a pH of 2.5. The optimal catalyst loading was 2000 mg/L; this loading led to the fastest degradation rate. It was also observed that an increase beyond 2000 mg/L did not affect the rate of degradation. Iron leaching tests were also conducted simultaneously with catalyst loading. At the optimum catalyst loading, an iron leaching concentration of 2.3 mg/L was found. Iron leaching kinetics were best predicted using the Pseudo-Second-Order (PSO) kinetics model. Finally, the optimum H_2O_2 dose was 1.0 mM. At doses exceeding 1.0 mM, the reaction becomes inhibited and thus, the degradation rate decreases. Under optimal conditions, complete decolourisation was achieved following 45 minutes of reaction time.

The degree of mineralisation of the MO was determined through Total Organic Carbon (TOC) analysis. Experiments were carried out in cycles with stepwise addition of H_2O_2 every 60 minutes for five cycles. TOC decreased rapidly following the first cycle with a TOC of 62.95 %; thereafter, the TOC continually decreased more gradually with a final TOC of 40 % after five cycles. The presence of TOC in the sample indicates that intermediate organic compounds were still present in the solution. However, it was confirmed that the original pollutant, Methyl Orange, had been completely degraded by the reaction through Liquid Chromatography-Mass Spectrometry analysis (LC-MS). The intermediates remaining in the solution were hypothesised based on literature.

iii

The practical viability of using ilmenite as a catalyst was assessed in terms of iron leaching content based on the South African Water Quality Guidelines for different water use purposes. Although the use of ilmenite led to minimal iron leaching (3.5 mg/L), the amount was still unsuitable for irrigation purposes because it could to rusting with the iron in solution becoming oxidised to form precipitates on metal surfaces; however, the iron content remains suitable for domestic usage as it is unlikely to cause any health effects at these concentrations for drinking and also poses no toxicity level for plants.

This study proves that ilmenite can be an effective catalyst in Fenton-like processes to degrade organic, aromatic compounds with minimal iron leaching. Future work should investigate the degradation intermediates of methyl orange in this system and evaluate suitable iron removal methods.

Keywords: Ilmenite, Fenton Reagent, Catalysis, Oxidation, Aromatic compounds, Wastewater Treatment

DECLARATION

I, Alicia Levana Butt, declare that the dissertation, which I hereby submit for the degree MSc. (Applied Sciences) in Environmental Technology at the University of Pretoria, is my own work and has not previously been submitted by me for a degree at this or any other tertiary institution.

SIGNATURE: *Alicia Levana Butt*

DATE: 28 September 2021

DEDICATION

To my parents, brother and life partner

Warren and Charmaine Butt, Wesley Butt and Wade Dorling

For their continuous support, encouragement and love

And

To my long term mentor, **Christiaan de Jager,** who first sparked my interest in environmental chemistry

ACKNOWLEDGEMENTS

TABLE OF CONTENTS

LIST OF FIGURES

LIST OF TABLES

ABBREVIATIONS

AOP   Advanced Oxidation Process

BET   Brunauer, Emmett and Teller (Surface Area)

BOD   Biological Oxygen Demand

COD   Chemical Oxygen Demand

CWPO   Catalytic Wet Peroxide Oxidation

DWAF   Department of Water Affairs and Forestry (now DWS)

DWS   Department of Water and Sanitation (South Africa)

EDS   Energy Dispersive X-Ray Spectroscopy

Fe   Iron

Fe (II)   Ferric Iron; Iron (II); Fe^{2+}

Fe (III)   Ferrous Iron; Iron (III); Fe^{3+}

$FeTiO_3$ Ilmenite

H_2O_2 Hydrogen Peroxide

H_2SO_4 Sulphuric Acid

HPLC   High-Performance Liquid Chromatography

IC   Ion Chromatography

ICP-OES Inductively Coupled Plasma Optical Emission Spectrometry

LC-MS   Liquid Chromatography-Mass Spectrometry

LOI   Loss on Ignition

MO   Methyl Orange

PFO	Pseudo-First-Order
POP	Persistent Organic Pollutant
PSO	Pseudo-Second-Order
SAWQG	South African Water Quality Guidelines
SEM	Scanning Electron Microscopy
TDS	Total Dissolved Solids
TiO_2	Titanium Dioxide; Rutile
TOC	Total Organic Carbon
UVA	Ultraviolet A (315-400 nm)
UVB	Ultraviolet B (280-315 nm)
WWTW	Wastewater Treatment Works
XRD	X-Ray Diffraction
XRF	X-Ray Fluorescence

LIST OF SYMBOLS

λ	Wavelength (nm)
a.u.	Arbitrary Unit
θ	Theta
$\bullet$	Radical species
e^-	Electron
h^+	Hole
nm	Nanometres
$\varepsilon_0[V]$	Standard Electrode Potential
m/z	Mass to charge ratio
k	Rate constant
t	time
C	Concentration at time t
C_0	Initial concentration

RESEARCH OUTPUTS

Journal Articles

1. Butt, A. L., Tichapondwa, S. M. (2020). Catalytic Wet Peroxide Oxidation of Methyl Orange using Naturally-Occurring South African Ilmenite as a Catalyst. Chemical Engineering Transactions, 81, 367-372. https://doi.org/10.3303/CET2081062

2. Butt, A., Kabangu, M., Tichapondwa, S. (2022). Photo-Fenton Oxidation of Methyl Orange Dye using South African Ilmenite Sands as a Catalyst. Catalysts, Special issue: Application of Photocatalysts in Environmental Chemistry.

Conference Presentations

1. Catalytic Wet Peroxide Oxidation of Methyl Orange using Naturally-Occurring South African Ilmenite as a Catalyst. 23rd Conference on Process Integration, Modelling, and Optimisation for Energy Saving and Pollution Reduction (PRES'20). 17th – 21st August 2020, Xi'an, China. (Oral Presentation).

2. South African Ilmenite as a naturally-occurring catalyst for wastewater treatment. Water Institute of Southern Africa Biennial Conference and Exhibition (WISA 2020). 7th – 11th December 2020, Online Conference. (PowerPoint Presentation).

1 CHAPTER ONE: INTRODUCTION

1.1 Background

Water scarcity has become an ever-growing concern within South Africa and globally (Oller et al., 2011, Water Research Commission, 2014). The continuous increase in population has put significant pressure on the worlds limited water resources, thus generating the need for clean, good quality water. Water is one of the most active substances on our planet, required not only to sustain life but needed for an endless variety of purposes such as ecological habitats, biological processes and climate. There is a high demand for good quality portable water; however, clean, quality water is not renewable. A significant volume of clean, drinking water is collected from underground aquifers through boreholes which can be depleted if over abstracted (Othman et al., 2018). One of the options to ensure a continual supply of clean water is through wastewater treatment that can generate water suitable for reuse.

Water is a fundamental carrier substance that allows for its functionality; however, this property also allows it to become easily contaminated. Many anthropogenic processes make use of large quantities of water, such as manufacturing and crop production. These large-scale industrial activities generate large quantities of effluent streams polluted with organic and inorganic pollutants. Organic pollutants such as aromatic and phenolic compounds are of particular concern as many of these compounds are known endocrine disruptors and carcinogens (Hai, 2007, Walker, 2009). Conventional biological wastewater treatment methods are the most widely used in wastewater treatment (Qasim and Zhu, 2018a). However, these processes are incapable of degrading priority and some emerging pollutants. As a result, water treatment processes such as adsorption (Jelic et al., 2015) and membrane separation have been implemented to make the effluent suitable for reuse. Although somewhat successful, these modern methods can generate secondary waste streams that require further treatment or specialised containment. Further treatment increases the cost of wastewater treatment processes and makes them challenging to implement in more impoverished communities. Due to the high stability of these phenolic organic pollutants, it has been challenging to identify cost-effective and sustainable methods of purifying such wastewater.

Over the past few decades, research into water purification has opened up new avenues for treating water containing organic pollutants. New technological developments such as Advanced Oxidation Processes (AOPs) have further increased the potential of water reuse due

to their ability to break down and mineralise refractory organic compounds. The predominant mechanism of AOPs is to generate highly oxidative free radical species that react with organic compounds, breaking them down into their most basic, inorganic forms such as carbon dioxide (CO_2) and water (H_2O), along with other inorganic elemental species (Ameta and Ameta, 2018). These highly oxidative species are generated through a variety of ways, such as light radiation (Photocatalysis), oxygen (Ozonation), sonar (Sono) and redox reactions (Fenton's Reaction). One of the most effective AOPs is Fenton's Reaction. This reaction makes use of an iron (Fe) salt and hydrogen peroxide (H_2O_2) to generate the highly reactive hydroxyl (•OH) radicals. The effectiveness of this method has led to new research and improvements on the original method; these improved methodologies are known as Fenton-like reactions (Fenton, 1894, Walling, 1975, Wang et al., 2016, Youssef et al., 2016). All of the Fenton-like reactions stem from the same principle as the original but investigate different parameters and additions to increase the efficiency and viability of the actual process.

1.2 Problem Statement

Fenton-like reactions are highly efficient in breaking down and mineralising organic compounds, although there are sometimes drawbacks. One of the main issues with the original Fenton's Reaction is that the Fe salt is highly soluble, leading to the generation of waste sludge which is high in Fe content. The high Fe content will need to undergo further treatment as such levels are unsuitable for most reuse purposes as it exceeds that which is considered safe to drink, and the high Fe concentration could lead to the rusting of pipes if used for irrigation purposes (CSIR Environmental Services, 1996a). Investigations began to identify solutions to this problem. One of the best solutions was to use a catalyst with low solubility but high redox potential that could also withstand the extreme conditions needed to activate the Fenton's Reaction (García-Muñoz et al., 2016a, Munoz et al., 2017, Ameta et al., 2018a, Tehrani-Bagha and Balchi, 2018). A focus on a solid phase, redox-active catalyst with low solubility increased. Many catalysts have made use of redox-active transition metals such as iron, manganese (Mn), copper (Cu) and zinc (Zn). There has been plenty of research into developing and investigating different catalysts from naturally occurring minerals to synthesised and modified materials. The use of a solid catalyst in Fenton-like reactions has become broadly known as the Heterogeneous Fenton-like Reaction.

When examining different catalysts, a focus also must be made to ensure the catalyst is efficient and non-toxic. A new interest in greener, cleaner technology has been on the rise, leading to

investigations into using naturally occurring compounds or minerals as catalysts and moving away from costly, synthesised materials.

The most effective of these materials are those containing redox-active elements, namely transition metals. Iron oxides have been most commonly used due to their sheer abundance and high redox potential. Ilmenite ($FeTiO_3$) is a cheap and highly abundant mineral found in South Africa and globally that has been shown to have catalytic potential (García-Muñoz et al., 2016a). Ilmenite is often mined as a source for titanium dioxide (TiO_2) and is considered the raw ore form of TiO_2. TiO_2 is a common material employed in another popular AOP, photocatalysis, whereby upon exposure to light generates electron/hole pairs that act as oxidising and reducing agents capable of degrading organic compounds (Ameta et al., 2018b). Ilmenite as a material contains both titanium and iron and thus can be an effective catalyst across a variety or combination of advanced oxidation processes. However, being naturally sourced, South African ilmenite might differ widely from the ilmenite used in similar research.

1.3 Aim and Objectives

This study aimed to investigate the effectiveness of using naturally occurring ilmenite as a catalyst in a Fenton-like reaction. This was applied in the degradation of phenolic pollutants. Methyl Orange (MO) was chosen as the target pollutant of this study due to its stability and inability to be degraded through conventional biological treatments. Methyl orange is furthermore an ideal candidate pollutant as it is an azo dye that, when degraded, will lose its colour properties. The objectives of this work are as follows:

- To characterise the chemical and physical characteristics of the raw ilmenite catalyst.
- To investigate the catalytic activity of the ilmenite in a Fenton-like process.
- To optimise the experimental conditions in terms of pH, light, catalyst loading and H_2O_2 dose.
- To assess the amount of Fe leaching into the solution.
- To model the kinetic parameters of the methyl orange degradation.
- To determine the extent of mineralisation of methyl orange.
- To evaluate the practical viability of using ilmenite as a catalyst in a Fenton-like reaction.

1.4 Dissertation Structure

Chapter 1: Introduction

Chapter 1 provides a brief overview of the aims and objectives of this research and provides background information on the problem at hand.

Chapter 2: Literature Review

This chapter provides an in-depth review of current and previous literature associated with wastewater treatment, AOPs and catalytic materials for removing organic contaminants in wastewater.

Chapter 3: Materials and Methods

The methods and materials used throughout this study are described in Chapter 3. Methods and materials of catalyst characterisation, degradation studies and analytical methodology are discussed in detail.

Chapter 4: Catalyst Characterisation

The results from the catalyst characterisation are described in terms of chemical and physical characteristics in this chapter. Postulations are also made regarding the potential impact on the catalyst's efficiency in the Fenton-like process.

Chapter 5: Degradation Studies

The catalytic activity of the catalyst in a Fenton-like process is investigated in this chapter through degradation studies. This chapter also investigates the effects of pH, irradiation, catalyst loading and hydrogen peroxide dosage on the degradation rate. The chapter further assesses the iron leaching into solution regarding different optimisation parameters.

Chapter 6: Degradation Mechanism

The extent of mineralisation and degradation of methyl orange using the ilmenite catalyst is assessed using TOC and LC-MS. The degradation kinetics and potential intermediate compounds are also examined.

Chapter 7: Practical Viability

Chapter 7 assesses the results of this research in terms of practical viability and real-world application. This chapter focuses on the usability of ilmenite in terms of cost of application and end product.

Chapter 8: Conclusion and Recommendations

The last chapter provides a summary of the research and presents conclusions based thereof. Recommendations for future research are also suggested.

2 CHAPTER TWO: LITERATURE REVIEW

2.1 Introduction

The investigation into environmentally sustainable practices and technology has become one of the most forefront research areas in the modern world. The increasing population continually stresses our planet's limited resources, particularly life-sustaining resources such as food and water (Esteves et al., 2019, Valhondo and Carrera, 2019). In 2015 the United Nations General Assembly created a list of 17 Sustainable Development Goals (SDG's). The purpose of these goals was to strive to achieve a more sustainable future. These goals include zero hunger, quality education and clean water and sanitation; the goals are divided into smaller targets. Goal 6 is clean water and sanitation; target three of this goal is to improve water quality, wastewater treatment and safe reuse by 2030. This goal is where the current research ties in to contribute towards this target. Whilst great strides are being made in other necessary fields such as agriculture to ensure food security, water scarcity has become a looming problem and a potential future crisis. Some global cities, such as Cape Town, have already come close to approaching "Day Zero", a term used to describe when water availability for a city is so low that water will have to be rationed to its citizens (Heggie, 2018).

There is a high demand for discovering new water sources; however, these are also limited and non-renewable, particularly in countries like South Africa and India, where major water crises are looming threats (Heggie, 2018, National Institution for Transforming India et al., 2019). Another way in which to address the demand for clean, usable water is through water reuse. Water reuse involves treating wastewater to a specific standard acceptable for reuse purposes such as irrigation, domestic or drinking use.

2.1.1 Wastewater

Wastewater is any source of water that has been polluted or contaminated through human usage and consumption. The largest consumers of water resources are agricultural and industrial processes (Valhondo and Carrera, 2019). These waste streams contain various chemicals, wastes, and pathogens at a concentration that makes them unsuitable for human use, whether for drinking, domestic or even agricultural purposes. Water reuse aims to purify the water to a certain standard whereby it no longer poses an environmental or health risk and is seen as suitable for specific reuse purposes.

2.2 Wastewater Treatment

Wastewater Treatment Works (WWTW) use various treatments and methods to remove contaminants and pollutants from water (Hofman-Caris and Hofman, 2019). These treatments are usually broken down into three stages, primary treatment, secondary treatment and tertiary treatment, depending on the quality of the effluent. Primary treatment removes solid waste from the water, mainly involving physical separation and minor chemical processes (Abdel-Raouf et al., 2012, Riffat, 2013d). Secondary treatment follows primary treatment, whereby biological and chemical processes are used to remove organic pollutants and pathogens from wastewater (Riffat, 2013d). Tertiary treatment is applied following secondary treatment to remove pollutants that could not be removed in the secondary treatment stage and thus often uses methods established to remove specific contaminants (Riffat, 2013d).

2.2.1 Preliminary and Primary Treatment

Preliminary treatment is usually the first stage in wastewater treatment (Riffat, 2013d). This stage involves the physical removal of large solids, such as twigs, cloth and other debris, and grit or abrasive particles (Abdel-Raouf et al., 2012, Qasim and Zhu, 2018c). Preliminary treatment is done through screening and grit removal. Screening makes use of a porous material through which wastewater is filtered; these screens range from coarse openings (6 mm – 75 mm) to micro openings (0.25 mm – 0.004 mm) (Qasim and Zhu, 2018c). These screenings remove the bulk of large solids found in wastewater. Grit removal is used to remove finer solid particles, usually through gravity settling or centrifugal force (Qasim and Zhu, 2018b).

Primary treatment usually follows preliminary treatment but is often used as the first treatment stage depending on the effluent treated. Primary treatment, like preliminary treatment, is the physical removal of solids from the wastewater (Riffat, 2013d, Ameta and Ameta, 2018). The purpose of primary treatment is to remove suspended solids that are usually organic and contribute to a high biological oxygen demand (BOD) (Riffat, 2013a). In this stage, the most widely used technology is sedimentation, whereby particles are forcibly settled in sedimentation tanks (Abdel-Raouf et al., 2012). Suspended solids removal can be done by physical means through gravitational settling and centrifugal force, or chemically using flocculants to coalesce particles till they reach a mass at which they settle out of solution

(Riffat, 2013a). Overall preliminary and primary treatment removes approximately 35 % of the BOD in the effluent stream (Hopcroft, 2015).

2.2.2 Secondary Treatment

Secondary treatment occurs when a large portion of solid pollutants has been removed through preliminary and primary treatment. At this stage, most of the pollutants are dissolved or in aqueous phases, such as heavy metals and water-soluble compounds. The purpose of secondary treatment is to remove biochemical oxygen demand (BOD), pathogens and in some cases, nutrients (Riffat, 2013c, Valhondo and Carrera, 2019). This stage involves the biological treatment, classified into two main groups: suspended growth and fixed growth treatment (Riffat, 2013c). Suspended growth involves the suspension of microorganisms in a biological reactor using a stirring technique. The most common method of suspended growth is the activated sludge process and is used in most industrial and municipal wastewater treatment plants (Riffat, 2013c). In this process, wastewater continually flows through a bioreactor containing various microorganisms that use the organic material for growth and energy (Abdel-Raouf et al., 2012). This bioreactor is continually aerated to provide aerobic conditions for microbial activity to occur. The microorganism's break down organic matter to generate cell mass and waste products (Riffat, 2013c).

Fixed growth treatment uses a similar process for removing BOD, except in place of suspended microorganisms, the microorganisms are attached to an inert object such as a biofilm. Wastewater flows over the biofilm, and the microorganisms break down the organic matter (Riffat, 2013b). These secondary treatment processes remove an estimated 50 % of BOD and 85 % of Total Dissolved Solids (TDS) (Hopcroft, 2015). Although practical, these biological processes cannot remove some emerging and priority pollutants, particularly those resistant to biological degradation, such as organic dyes and some pharmaceuticals (Bandara et al., 1999, Devi et al., 2009). Following this stage is where tertiary treatment is usually applied.

2.2.3 Tertiary Treatment

Tertiary treatment is usually only applied when harmful or toxic levels of a substance still occur following conventional treatment. Tertiary or advanced treatment is mainly used to remove specific toxic compounds from the wastewater and disinfection potential pathogens (Riffat,

2013d). These treatments aim to remove specific nutrients, such as nitrogen, phosphorous and heavy metals or any other organic or inorganic compound of concern that could not be removed through secondary treatment (Riffat, 2013d). One of the main challenges in recent times is removing persistent and resistant organic compounds such as pesticides, dyes, pharmaceuticals and other persistent organic pollutants (POPs) (Hofman-Caris and Hofman, 2019). These compounds are often resistant to conventional wastewater treatment processes, such as biological and irradiation and need to undergo specialised treatments to mineralise into CO_2, H_2O and other inorganic constituents (Devi et al., 2009).

2.3   Advanced Oxidation Processes (AOPs)

Advanced Oxidation Processes (AOPs) are a group of technologies used to break down highly resistant and stable organic compounds, such as pharmaceuticals, dyes, pesticides and other emerging contaminants in wastewater (Ameta and Ameta, 2018). The primary mechanism of AOPs is the generation of oxidative species or radicals like the hydroxyl radical (•OH) (Oturan and Aaron, 2014). These radicals are highly reactive and can break down even the most stable compounds. The radicals oxidise the contaminant into smaller organic molecules and can lead to their complete mineralisation, whereby the contaminant is broken down into carbon dioxide (CO_2) and water (H_2O) (Wang et al., 2016). There are many different processes and methodologies used to generate such radicals, but the most popular and effective are the Fenton and Fenton-like Reactions, Catalytic Wet Peroxide Oxidation (CWPO) and photocatalysis. **Figure 1** shows a schematic classification of different AOPs based on the hydroxyl species generated in the process.
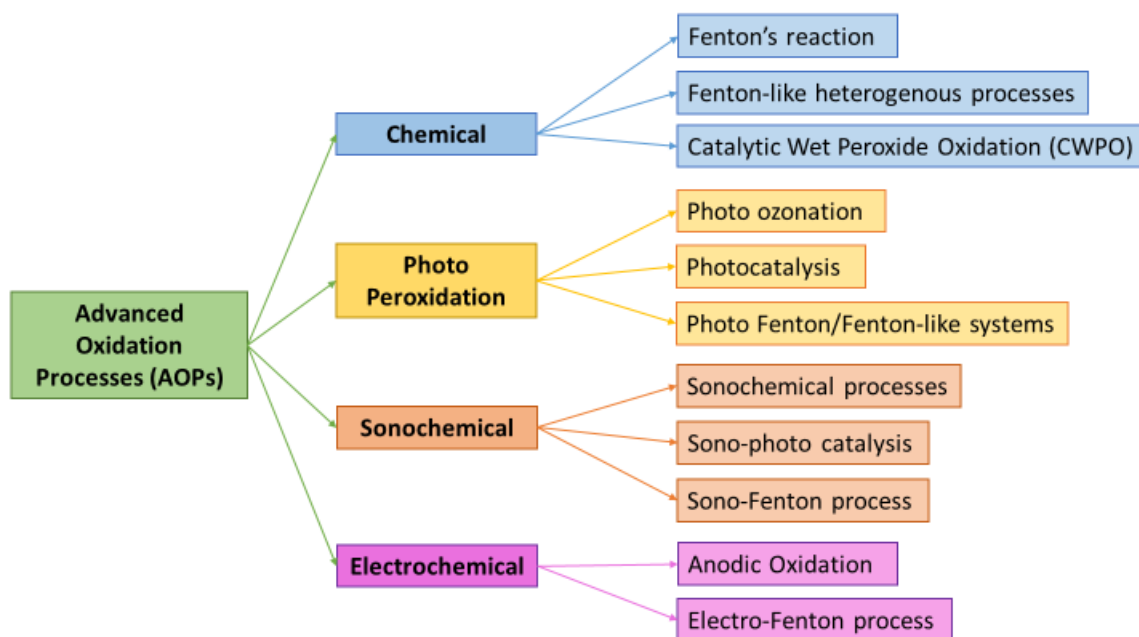
Figure 1:   Classification of AOPs based on the generation of hydroxyl species. Adapted from Kurian (2021)

AOPs are grouped according to the oxidative species generated, as seen above. The chemical AOPs make use of catalysts with high redox potential to generate radicals whilst the photo-, sono- and electro-AOPs make use of external energy (light, sonar, electrical) to activate the system. The AOPs of interest in this study are those that make use of chemical and photo means.

2.3.1   Fenton and Fenton-like Reactions

H. J. Fenton first developed the Fenton Reaction in 1894. This method entails the use of an iron (Fe (II)) salt as a catalyst and hydrogen peroxide (H_2O_2) at low pH values (< 4) to generate reactive radical species in solution to break down organic pollutants (Fenton, 1894). The Fenton Reaction is a highly effective and fast-acting method to break down complex organic compounds and was applied in various wastewater treatment operations (Wang et al., 2016). The original Fenton Reaction used a highly soluble iron salt; this led to secondary sludge with high iron content up to 80 mg/L in batch processes (Jafarinejad, 2017). The high iron concentration required using the iron salts has been the main downfall of the homogenous process (Robinson et al., 2001, Soon and JHameed, 2011, Ortiz et al., 2019). Not only does the

10

high Fe content make the effluent unsuitable for most reuse purposes but the Fe ions remaining in solution may interfere with the full mineralisation of organic compounds as Fe can chelate with short-chain organic acids to form metal-ligand complexes (Sparks, 2003a). The Fenton process is displayed through the following reactions (reaction (1) – (7)) adapted from (Walling, 1975, Barbusinski, 2009, Youssef et al., 2016):

$$Fe^{2+} + H_2O_2 \rightarrow Fe^{3+} + \bullet OH + OH^- \tag{1}$$

$$Fe^{3+} + H_2O_2 \rightarrow Fe^{2+} + \bullet OOH + H^+ \tag{2}$$

$$Fe^{3+} + \bullet OOH \rightarrow Fe^{2+} + H^+ + O_2 \tag{3}$$

$$\bullet OH + H_2O_2 \rightarrow \bullet OOH + H_2O \tag{4}$$

$$\bullet OH + Fe^{2+} \rightarrow Fe^{3+} + OH^- \tag{5}$$

$$\bullet OH + \bullet OH \rightarrow H_2O_2 \tag{6}$$

$$\bullet OH + \bullet OOH \rightarrow O_2 + H_2O \tag{7}$$

From this point, the free radicals will interact with the organic pollutants through hydroxylation, methylation and demethylation to cleave the intramolecular bonds (Dai et al., 2007).

Similar reactions have been developed to combat the limitations of the original process known as Heterogenous Fenton-like reactions. This group of reactions uses a solid, iron-bearing catalyst in place of a soluble catalyst to minimise iron leaching. The reason these reactions are called "Fenton-like" is that the mechanism of the reaction remains the same; however, different activation mechanisms can be used, such as light activation (Photo-Fenton), electrochemical activation (Electro-Fenton), microwave activation (Microwave-Fenton) and many other variations (Wang et al., 2016). A study conducted by Tokumura et al. (2011) suggests that Fenton-like reactions, particularly the Photo-Fenton reaction, have two main mechanisms that lead to the generation of •OH radicals (reaction (8) & (9)), with reaction 8 being the same primary reaction of the conventional Fenton process.

$$Fe^{2+} + H_2O_2 \rightarrow Fe^{3+} + \bullet OH + OH^- \tag{8}$$

$$Fe^{3+}(OH)^{2+} \xrightarrow{h\nu} Fe^{2+} + \bullet OH \tag{9}$$

11

This second reaction (reaction (9)) allows for the cycling between Fe (II) and Fe (III). The author concludes that the presence of UV light irradiation to the Fenton system is superior to the original Fenton reaction as it ultimately leads to the production of solely •OH radicals instead of the weaker •OOH radical (Tokumura et al., 2011).

2.3.2 Catalytic Wet Peroxide Oxidation (CWPO)

The Catalytic Wet Peroxide Oxidation (CWPO) is another AOP that has been introduced to overcome the problems associated with the Fenton reaction (Ameta et al., 2018a, Tehrani-Bagha and Balchi, 2018). This process uses a solid metal-bearing catalyst instead of a metal salt to avoid metal leaching and sludge formation. Although often called the CWPO process, many terms describe similar oxidative processes involving a solid catalyst and H_2O_2. One of the most commonly used alternative terms is the Heterogeneous Fenton-like Reaction, commonly used when the solid catalyst is iron-bearing (Esteves et al., 2019). The CWPO or Heterogeneous Fenton-like Reaction can be a sustainable and effective process for wastewater treatment, with minimal limitations and negative outputs. Current research in the field of AOPs today tends to focus on the nature of the catalysts being used in these systems, to identify efficient, fast and cost-effective catalysts to work in these systems to degrade a variety of emerging and priority pollutants. In this field of catalysis, there is a large focus on the type of catalysts being used. A review paper by Wang et al. (2016) focused on Fenton-like processes for wastewater treatment, focusing on catalysts types. Generally speaking, catalysts can be classified as natural and synthetic, with synthetic comprising a large group of different types. Composites are a type of synthetic catalytic material made of more than one type of material; they are of particular interest as they can be easily recovered from a solution through precipitation. These catalysts involve using a support, such as clay or carbon nanotubes with an active metal created through impregnation, which can be a costly process (Wang et al., 2016, Mak et al., 2021).

Recently emerging research has focused on identifying naturally occurring minerals as catalysts to combat these issues (Lu et al., 2002, García-Muñoz et al., 2016a, Munoz et al., 2017). Ilmenite ($FeTiO_3$) is one such mineral that has shown promise as a catalyst for AOPs. The presence of redox-active element Fe in the ilmenite structure allows it to be suitable for Fenton-like processes, whereas the presence of Ti indicates that the mineral could potentially have photocatalytic activity (García-Muñoz et al., 2016a).

12

2.3.3 Photocatalysis

Photocatalysis makes use of a semi-conductor material as a catalyst that is driven by exposure to irradiation. In this process, an electron-hole pair is generated on the material. When the catalyst is exposed to irradiation of a particular wavelength, in the valence band, an electrons absorbs the photon's energy and is excited to the conduction band (Ameta et al., 2018b). This causes the generation of an electron (e^-) and hole (h^+) pair. Photocatalysis creates an oxidising environment and a reducing environment, whereby the electron will reduce an acceptor, and the hole will oxidise a donor molecule (Ameta et al., 2018b). **Figure 2** gives a brief schematic of the three main AOPs discussed above.
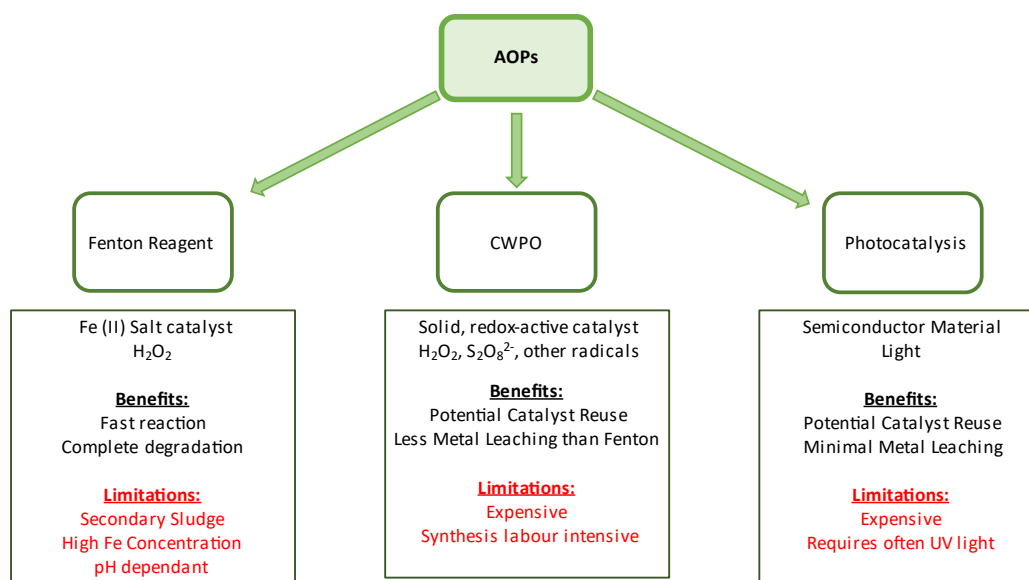
Figure 2: Most common AOPs with listed benefits and limitations to each method. Adapted from (Ameta et al., 2018a, Ameta et al., 2018b, Tehrani-Bagha and Balchi, 2018)

Across the various AOPs shown in **Figure 2**, it can be seen that the significant limitations of these methodologies are the high expense of their usage as well as the potential generation of harmful, secondary sludge. This research aims to address these limitations by using a catalyst that will be inexpensive and lead to little heavy metal leaching into the treated wastewater. Much research has been done on different catalysts and their relative efficiency at combating these limitations and effectively degrading priority and emerging contaminants.

13

2.4 Types of Catalysts for AOPs

A catalyst is any material that can activate or increase the reaction rate but is not consumed by that reaction. Historically the most popular catalysts used in AOPs are either iron-bearing (Fenton) or a semi-conductor material such as TiO_2 (Photocatalysis). In recent years many different catalysts have been used in AOPs, ranging from homogenous to heterogenous and from synthetic to natural. **Table 1** summarises recent studies in tertiary wastewater treatment similar to the research presented in this work in terms of catalyst, pollutant or process.

14

Table 1:   Different catalysts used in AOPs in previous studies

Compound / Material	Advanced Oxidation Process	Pollutant	Aim	Operating Conditions	Findings	Reference
Titanium Dioxide	Photocatalysis with solar irradiation	Methyl Orange	The study aimed to investigate the possibility of using solar radiation for the degradation of methyl orange using TiO_2	**Operating conditions:** pH = 3, [MO] = 0.04 mM, TiO_2 = 0.4 % ration (± 4 g/L)	The study found that using 0.4% TiO_2 gave a degradation rate of 0.639 h^{-1} under the influence of solar irradiation.	Al-Qaradawi and Salman (2002)
Titanium Dioxide (Polycrystalline suspension)	Photocatalytic oxidation with solar irradiation with H_2O_2 and $S_2O_8^{2-}$	Methyl Orange & Orange II (Azo-Dyes)	The study aimed to use a heterogenous photocatalytic system to oxidise two azo dyes; operating conditions were investigated. The influence of H_2O_2 and $S_2O_8^{2-}$ on the degradation of the dyes was also investigated.	**Operating conditions:** Catalyst = 0.2 g/dm^3, dye concentration = 5 to 50 ppm	**Photocatalysis only:** The study found higher mineralisation at pH 3 and 6.7. The study found complete disappearance of Methyl Orange at all concentrations and complete disappearance of Orange II only at concentrations of 20 ppm and lower. **H_2O_2 and $S_2O_8^{2-}$:** Reaction rates for both dyes increased in the presence of $S_2O_8^{2-}$. An increase in degradation rate was	Augugliaro et al. (2002)

Magnetite, Ilmenite & Hematite	Heterogenous Fenton / CWPO	Phenol (100 mg/L)	The study aimed to optimise the application of naturally-occurring iron based minerals as catalysts in the CWPO process	**Operating conditions:** pH = 3, $[H_2O_2]$ = 500 mg/L, Temp = 75 °C	Time = 4 hours (240 min) **Iron Leaching:** Magnetite: 13 mg/L, Ilmenite: 1 mg/L, Hematite: 3 mg/L	Munoz et al. (2017)
Alginate-Fe^{2+}/Fe^{3+} film	Heterogenous Fenton and Fenton-like processes	Methyl Orange	The study investigated the viability of Alg-Fe^{2+} and Alg-Fe^{3+} films as catalysts in the Fenton and Fenton-like processes using methyl orange as the pollutant.	**Operating conditions:** Volume = 250 ml, Catalyst = 60 mg, MO = 50 ml	H_2O_2 concertation above ten mM retarded the reaction.	Quadrado and Fajardo (2017)
Vanadium bearing Rutile	Photocatalysis with and without H_2O_2	Methyl Orange	The study aimed to determine the possibility of using natural rutile (containing V^{5+} and Fe^{3+}) as a photocatalyst in visible light with and without the addition of H_2O_2.	**Operating Conditions:** Catalyst = 1 g/L, [MO] = 11.307 mg/L, $[H_2O_2]$ = 3.8 mM, Irradiation = 300 nm	The study conducted three experiments: 1) rutile only, 2) rutile and H_2O_2, 3) rutile with H_2O_2 and irradiation. The study found the highest decolouration of DB3 (60.59%) in the presence of H_2O_2 and	Lu et al. (2007)

					irradiation after 60 min of reaction time.	
Zero valent metallic iron (Fe)	Fenton process & Photo-Fenton Process	Methyl Orange	The study aimed to investigate the effectiveness of using zero valent Fe as a source of Fe (II) ion production in a Fenton oxidation process. The influence of operating parameters was investigated.	**Operating Conditions:** pH = 2.0 to 9.2, Fe (0) = 10 mg/L to 200 mg/L, $[H_2O_2]$ = 2 ppm to 20 ppm, Temperature = 25 °C, Irradiation = 350 nm – 400 nm.	**Optimal Operating Conditions:** pH = 3, Fe (0) = 10 mg/L, [MO] = 10 ppm, $[H_2O_2]$ = 10 ppm, Temperature = 25 °C, Irradiation = 350 nm – 400 nm. Discolouration of the dye was achieved in 15 min under optimal conditions. Iron leaching was found to be 2.78×10^{-3} M.	Devi et al. (2009)
Mesoporous titania nanoparticles	Photocatalysis	Methyl Orange	The study aimed to investigate the effect of photocatalytic conditions on the efficiency of the degradation of methyl orange.	**Operating Conditions:** pH = 2, Catalyst = 1 g/L, Irradiation = 365 nm, [MO] = 20 ppm	Methyl Orange mineralisation of 98 % was achieved after 45 min of irradiation.	Dai et al. (2007)
Zinc Oxide (ZnO)	Photocatalysis	Acid red 14 (azo dye)	The study aimed to study the photocatalytic degradation of acid red 14 (AR14) using ZnO as an alternative catalyst to TiO_2.	**Operating Conditions:** pH = neutral, AR14 = 20 ppm, ZnO = 160 ppm, Irradiation = UV-C (100 nm – 280 nm)	Complete decolourisation was achieved in 60 min under the optimal operating conditions.	Daneshvar et al. (2004)

CuFe$_2$O$_4$-Fe$_2$O$_3$	Photocatalysis and Heterogenous Photo-Fenton	Methylene blue (MB)	The study aimed to synthesise mixed copper and iron oxides for application in the heterogenous photo-Fenton reaction under solar light.	**Operating Conditions:** [MB] = 10 to 50 mg/L, catalyst = 1 g/L, pH = 3; 6, [H$_2$O$_2$] = 100 mg/L; 300 mg/L, Irradiation = natural solar light	The catalyst did not show any activity in the absence of H$_2$O$_2$. In its presence, 100% removal of the dye was achieved in 180 min. The reaction had a kinetic constant of 0.016 min^{-1}.	Silva et al. (2020)
Hematite (α-Fe$_2$O$_3$)	Photo-Fenton-like process	Methyl Orange	The study aimed to determine the effect of different additives on the morphology and structure of α-Fe$_2$O$_3$. Methyl orange was used as a pollutant to assess the photocatalytic activity of the hematites in the presence of UV irradiation.	**Operating Conditions:** Catalyst = 1 g/L, [MO] = 2.5 ppm, Irradiation = UVC (λ = 253.7 nm), [H$_2$O$_2$] = 1 μL/mL. Three α-Fe$_2$O$_3$ catalysts were prepared with the following additives: a) NaCl, b) Na$_2$SO$_4$, c) Na$_2$C$_2$O$_4$	The morphology created when the Fe$_2$O$_3$ was prepared using Na$_2$SO$_4$ created an urchin-like structure. This morphology displayed the highest photocatalytic activity with 76.5 % removal of 2.5 ppm methyl orange following 2 hours of irradiation. The authors attributed this to the high surface area of the created morphology.	Domacena et al. (2020)
Natural Soil (Warangal region in Tamil Nadu, India)	Photo Fenton-like Process	Pharmaceuticals: Ornidazole (ORZ) & Ofloxacin (OFX)	The study aimed to utilise naturally available soil as a catalyst in a photo-Fenton-like process for treating pharmaceuticals in wastewater in batch and continuous systems. The	**Optimal Conditions:** ORZ: pH = 3, Soil = 0.033 g/L, H2O2 = 1 mM, Irradiation = Solar	**Soil Characterisation:** Major soil components were Fe (37.13 %), Al, Si, K, C, Mg and Ca. Hematite, magnetite, goethite, pyrite and wustite were main oxide minerals.	Changotra et al. (2017)

				OFX: pH = 3, Soil = 0.020 g/L, H_2O_2 = 2 mM, Irradiation = Solar	**Degradation:** The study found no degradation using H_2O_2 or solar light alone after 60 min. Both compounds were effectively degraded in the presence of both H_2O_2/Solar light and H_2O_2/UV irradiation. Under optimal conditions, 98 % and 95 % removal were achieved for ORZ and OFX, respectively.	
			effects of catalyst loading, pH, H_2O_2 dose and irradiation (UVA, UVB, Solar) were examined.			
Ilmenite	CWPO-Photoassisted process	Phenol (100 mg/L)	Using solar light irradiation, the study investigated the feasibility of using ilmenite as a low-cost catalyst for the CWPO process.	**Operating Conditions:** pH = 3, $[H_2O_2]$ = 500 mg/l, Catalyst = 450 mg/L, Temperature = 25 °C, UV = 320 nm	**Absence of Irradiation:** The study found that conducting experiments without solar irradiation had a 3-hour induction period before any degradation occurred. TOC conversion was 50 % after 480 min. Iron leaching was 2.3 mg/L **Solar Irradiation:** Total phenol and H_2O_2 conversion were achieved within 480 min with a TOC conversion of 95 %.	García-Muñoz et al. (2016a)

Ilmenite	UV-LED/FeTiO$_3$ oxidation process	Disperse Blue 3 (DB3) (80 mg/L)	The study aimed to assess the degradation of DB3 using a UV-LED/FeTiO$_3$ system using persulfate (S$_2$O$_8$$^{2-}$) as the primary oxidant species. The study also focused on the optimisation of the operating parameters.	**Operating Conditions:** pH = 3, Persulfate = 1.7 g/L to 0.34 g/L, ilmenite = 150 mg/L to 450 mg/L, Irradiation = 405 nm, Temperature = 30 °C to 70 °C	**Optimal Conditions:** Ilmenite = 320 mg/L, [S$_2$O$_8$$^{2-}$] = 1.56 g/L, Temperature = 67 °C. Under optimal conditions, 96 % mineralisation was achieved after 180 min.	Silveira et al. (2018)

2.4.1 Ilmenite as a Catalyst for AOPs

Studies conducted over the past several years have aimed at identifying efficient, cost-effective catalysts for use in AOPs (Oh et al., 2009, Teel et al., 2011, Wang and Chu, 2012, Carbajo et al., 2014, Hadjltaief et al., 2014, Munoz et al., 2015, Pliego et al., 2015, Pliego et al., 2016, Munoz et al., 2017). Among research in this field is an interest in using ilmenite ($FeTiO_3$) as a heterogenous catalyst (García-Muñoz et al., 2016a, García-Muñoz et al., 2016b, García-Muñoz et al., 2017a, García-Muñoz et al., 2017b, Silveira et al., 2017, García-Muñoz et al., 2018, Silveira et al., 2018).

Ilmenite is an iron-titanium oxide that occurs naturally in soils and sands with the stoichiometric formula of $FeTiO_3$ with iron in its ferrous (Fe (II)) and ferric form (Fe (III)) and titanium in its tetravalent form (Ti (IV)). Ideally, ilmenite has a composition of 36.8 % iron, 31.6 % titanium and 31.6 % oxygen; however, natural ilmenite may contain trace amounts of manganese and magnesium through substitution. Ilmenite has also been found to contain Hematite (Fe_2O_3), although at a weight percentage below six (Klein and Dutrow, 2007). Ilmenite has a hexagonal crystalline system similar to that of corundum, in which the iron and titanium atoms are ordered in alternating octahedrally coordinated layers (Klein and Dutrow, 2007). The presence of ferric and ferrous iron in the ilmenite matrix, as well as a titanium content, allows for the reasonable assumption that ilmenite may be an alternative catalyst for the treatment of wastewater in AOPs. Previous studies have shown that light (300 nm to 450 nm UV light) influences the Fe (III)/Fe (II) redox cycle, promoting and increasing the degradation of organic pollutants in what is termed the Photo-Fenton reaction or the CWPO-Photoassisted process (Fallmann et al., 1999, Wang and Chu, 2012, Hadjltaief et al., 2014, Minella et al., 2014).

A study conducted by García-Muñoz et al. (2016a) sought to investigate the viability of using ilmenite as a catalyst for the CWPO in combination with photocatalysis. The experiments were carried out in a weathering chamber using ilmenite as a catalyst and phenol as the contaminant. The system was in the presence of hydrogen peroxide and exposed to an irradiation source simulating solar light (García-Muñoz et al., 2016a). Photocatalytic runs were conducted using ilmenite, and titanium dioxide was used as reference material. It was found that at low pH values (pH 3), the titanium dioxide and the ilmenite showed similar photoactivity; however, the activity of the titanium dioxide was significantly higher at a pH of 6. The authors attributed

the low photo activity of the ilmenite to the presence of Fe (II) and Fe (III) that behave as electron/hole scavengers leading to a decrease in the generation of hydroxyl radicals (•OH). Another reason for this may be the high Fe/Ti molar ratio that leads to electron/hole pair recombination, causing a loss of energy in the process (García-Muñoz et al., 2016a). CWPO runs were also conducted using ilmenite as a catalyst. The study found that after a 3-hour induction period, there was negligible variation in the phenol and hydrogen peroxide concentrations. The authors suggest that this indicates that the ilmenite needs to be activated to generate hydroxyl radicals through the decomposition of hydrogen peroxide (García-Muñoz et al., 2016a). The authors concluded that there are limitations to using ilmenite as a photocatalyst or a catalyst in the CWPO process but suggest that the high induction time and low oxidation rate from the CWPO can be overcome with the inclusion of light irradiation in a process called the CWPO-Photoassisted process (García-Muñoz et al., 2016a). The study found that this combination process (conducted at a pH of 3 and temperature of 25 °C) reduced the total organic carbon (TOC) to below 10 % with total phenol and hydrogen peroxide conversion within a 480 minutes reaction time (García-Muñoz et al., 2016a). The suggested mechanism is as follows: (1) Electron/hole pairs were generated by irradiating ilmenite and (2) these electron/hole pairs reacted with the H_2O_2 to generate •OH and •OOH radicals (García-Muñoz et al., 2016a). Aromatic intermediates, short-chain acids, were detected in the reaction solution as the reaction progressed. The concentration of leached iron was found to be low, indicating the stability of the catalyst. The catalyst, ilmenite, was used for a further five runs with rinsing off the catalyst in-between with the final run resulting in a TOC conversion of above 90 % (García-Muñoz et al., 2016a). Similar results have also been found by García-Muñoz et al. (2017b), where the CWPO-Photoassisted process combined with an ilmenite catalyst was used for the treatment of hospital wastewater. The experiments involved two CWPO-Photoassisted runs, one using simulated hospital wastewater using sulfadimethoxine (antimicrobial medication) as a contaminant and the other using real hospital wastewater (García-Muñoz et al., 2017b). The study found TOC and chemical oxygen demand (COD) conversions of 80 % each (García-Muñoz et al., 2017b).

Although the CWPO-Photoassisted process showed promise using ilmenite as a catalyst, the catalytic activity of the ilmenite was still lower than that of other heterogenous catalysts (García-Muñoz et al., 2016a, García-Muñoz et al., 2016b). Solutions to this limitation were addressed in further research by some of the same authors in García-Muñoz et al. (2016b). This study aimed to use a Temperature Programmed Reduction (TPR) to vary the Fe (II)/Fe (III)

22

ratio on the ilmenite surface to increase the number of reduced iron species. The experimental procedure differed from the study mentioned above, García-Muñoz et al. (2016a), by using Light Emitting Diodes (LEDs) instead of simulated solar light radiation (García-Muñoz et al., 2016b). The purpose of the study was to assess the effect of reduction treatment on the physical, chemical and catalytic properties of ilmenite using phenol as a contaminant (García-Muñoz et al., 2016b). The raw catalyst was subjected to a reduction in an H_2 atmosphere before the CWPO-Photoassisted runs, two changes in iron oxidation state were observed as follows: (1) the partial reduction of Fe (III) to Fe (II) at 500 °C and (1) the reduction of Fe (II) to Fe at 950 °C. These two catalysts obtained were deemed reduced ilmenite (500 °C) and highly reduced ilmenite (950 °C). The three solids (raw ilmenite, reduced ilmenite and highly reduced ilmenite) were used in the CWPO-Photoassisted runs (García-Muñoz et al., 2016b). All three catalysts showed total degradation of H_2O_2 in 240 min with the highly reduced ilmenite reaching total decomposition first just under 100 min (García-Muñoz et al., 2016b). In all scenarios, the TOC reduction was close to 95 %. The faster reaction time of the highly reduced ilmenite was explained via the following mechanism: (1) Fe reacted with H_2O_2 to generate •OH radicals and Fe (III) and finally (2) the Fe was able to reduce the generated Fe (III) to Fe (II) creating a closed loop that continued until total H_2O_2 was decomposed. However, the reduced and highly reduced catalysts displayed other problematic consequences, the reduction of the catalyst was found to alter its stability and lead to an increase in iron leaching, although minimal at 3 % of total iron in the catalyst (García-Muñoz et al., 2016b). Long-term continuous experiments were conducted on the three catalysts where a solution of phenol and H_2O_2 were continuously fed into the reactor. It was found all three catalysts maintained a high stability with almost 100 % TOC conversion up to 50 hours thereafter a steep deactivation was seen, with catalyst stability decreasing with an increase in ilmenite reduction (García-Muñoz et al., 2016b).

A study conducted by Silveira et al. (2017) also investigated the use of ilmenite as a catalyst for wastewater treatment, specifically focusing on the dye Disperse Blue 3 (DB3) as the research contaminant. The study investigated the use of ilmenite as a catalyst for persulfate activated AOPs instead of H_2O_2 activated AOPs (Silveira et al., 2017). The main difference between using persulfate versus hydrogen peroxide is the radicals generated; using persulfate generates •SO_4^- radicals whereas hydrogen peroxide generates •OH radicals (Oh et al., 2009, Silveira et al., 2017). The use of persulfate in the successful degradation of dyes has been previously studied (Oh et al., 2009, Xu and Li, 2010, Kordkandi and Forouzesh, 2014). A study

23

conducted by Teel et al. (2011) examined the use of thirteen naturally occurring minerals to activate (decompose) persulfate, amongst the minerals that showed a higher rate of persulfate decomposition was ilmenite; other minerals giving similar results included cobaltite, pyrite and siderite (Teel et al., 2011). The experiment conducted by Silveira et al. (2017) used a process similar to the CWPO-Photoassisted process but with persulfate and UV-LED light in place of H_2O_2 and solar light.

Furthermore, the experiments were conducted over a range of temperatures from 30 to 70 °C with the presence and absence of LED light (Silveira et al., 2017). The ilmenite catalyst was reused for three runs. The ilmenite was filtered out of the system and dried overnight at 60 °C (Silveira et al., 2017). In the absence of light and ilmenite, the activation of persulfate was little at temperatures below 50 °C but increased to 39 % TOC removal at a temperature of 70 °C. With the addition of ilmenite as a catalyst at 70 °C, the TOC removed was around 55 %. The system using UV-LED, ilmenite and heat (70 °C) showed a TOC removal of close to 96 %. A comparison experiment using UV-LED, heat and TiO_2 in place of ilmenite generated a TOC removal of 82 %. Although the authors do not state a reason for ilmenite performing better than titanium dioxide in a UV-LED/persulfate/heat system, the assumption is that iron ions in the ilmenite structure lead to the generation of more potent radicals ($\bullet SO_4^-$). The study also observed that the mineralisation of the dye decreased with each consecutive use of the ilmenite catalyst, which indicated the loss of catalyst stability with each run (Silveira et al., 2017). The authors postulated that the reason for this deactivation is (1) the loss of iron through leaching, although only in minute amounts, and (2) the deposition of SO_4^- upon the surface of the ilmenite generating $FeSO_4$ and $Fe_2(SO_4)_3$ on the ilmenite surface (Silveira et al., 2017).

Further research conducted by García-Muñoz et al. (2017a) aimed to investigate the use of ilmenite as a catalyst in CWPO, photocatalysis and CWPO-Photoassisted process for the degradation of sulphonamide antibiotics. The experiments were carried out similarly to that of García-Muñoz et al. (2016a), using sulphonamide as a contaminant in place of phenol. The study found that photocatalysis and the CWPO-Photoassisted process both resulted in the complete removal of sulphonamide. However, the photocatalysis method resulted in 35 % TOC removal, whereas the CWPO-Photoassisted process resulted in an 85 % TOC removal (García-Muñoz et al., 2017a). This difference in TOC removal was attributed to different reaction mechanisms at play where oxidation via photocatalysis occurs through radical condensation, which generates high molecular weight by-products and through CWPO-Photoassisted process

through hydroxylation generates low molecular weight by-products (García-Muñoz et al., 2017a). The study concluded that the use of ilmenite as a catalyst for the CWPO-Photoassisted process could be an efficient alternative to wastewater treatment (García-Muñoz et al., 2017a). Furthermore, the study found that in the reuse of the ilmenite catalyst after three consecutive runs, the catalyst maintained its efficiency and stability (García-Muñoz et al., 2017a). This finding and previous findings (García-Muñoz et al., 2016a, García-Muñoz et al., 2016b, García-Muñoz et al., 2017b) show that the use of H_2O_2 in AOPs has little to no effect on the stability of the catalyst, unlike the use of persulfate that leads to catalyst deactivation (Silveira et al., 2017).

Finally, in the latest study by García-Muñoz et al. (2018), the effect of light on the CWPO process was studied using two pH levels, acid (pH 3) and neutral (pH 6) using ilmenite as a catalyst and phenol as a contaminant. The CWPO process was carried out in dark and light conditions with UV radiation, with two solution pH values. Furthermore, the stability of the ilmenite catalyst was also evaluated over several consecutive runs (García-Muñoz et al., 2018). The CWPO run conducted in the absence of light revealed the effect of pH on phenol degradation. The experiments conducted in the absence of light showed that at the neutral pH of 6 after 480 minutes, the total phenol reduction was less than 30 % with negligible TOC removal, whilst total phenol conversion was observed at a pH of 3 after 480 minutes with TOC removal of 50 %. The CWPO in the presence of light yielded more efficient results with 100 % phenol and TOC removal, the acidic pH value of 3 yielded these results in 240 minutes, whilst the neutral pH yielded these results in 360 minutes (García-Muñoz et al., 2018).

In light of the studies mentioned above, it is reasonable to assume that using ilmenite as a catalyst for AOPs might provide an efficient alternative to modern wastewater treatments and potentially reduce the cost estimation of such treatments. The CWPO-Photoassisted process and well as Fenton-like reactions using ilmenite has shown considerably positive results. However, as detailed above, most of the research has used purified ilmenite forms, whereas this study uses raw, natural ilmenite.

2.5 Summary

In most existing wastewater treatment plants, wastewater is processed by physical, chemical, and biological purification systems. However, most conventional processes cannot degrade

some priority and emerging compounds such as dyes and pharmaceuticals. Advanced Oxidation Process provides a solution to the degradation of highly stable compounds. Many popular AOPs such as the Fenton reagent, catalytic wet peroxide oxidation and photocatalysis have soon promise as a means to degrade these compounds. Research into these processes has found that combination processes, such as the Fenton-like reactions, can behave more efficiently than the processes alone. The Fenton-like processes make use of an iron-bearing catalyst and H_2O_2 to generate free radical species. Current research is focused on identifying and synthesising suitable, effective catalysts for this process. **Figure 3** shows the benefits and limitations associated with using naturally occurring catalysts versus synthetic catalysts.
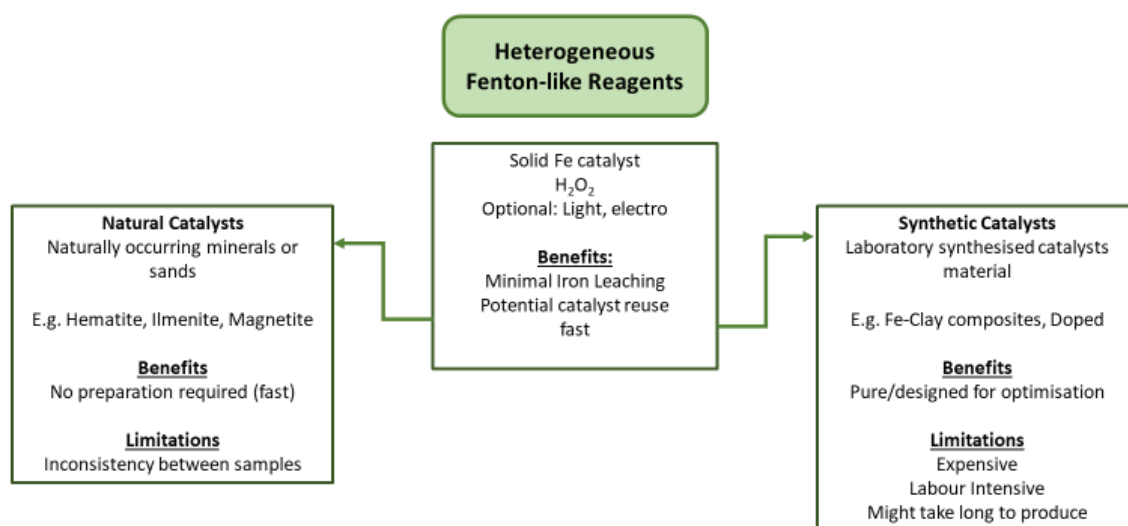
Figure 3:   Benefits and Limitations of using natural versus synthetic catalysts. Adapted from (García-Muñoz et al., 2016a, Wang et al., 2016, Munoz et al., 2017)

This work investigates naturally occurring ilmenite as a catalyst in a heterogenous Fenton-like process to degrade the highly stable methyl orange azo dye. Ilmenite presents as a promising catalyst due to the high iron concentration of the mineral. The mineral also contains titanium which might allow it to present photocatalytic properties. Catalyst characterisation and process optimisation were carried out to determine the role of ilmenite in the degradation process.

3 CHAPTER THREE: MATERIALS AND METHODS

3.1 Materials

Pre-milled (< 54 μm) ilmenite was supplied by AMIS Matrix Reference Materials (AMIS 0454). The ilmenite was sourced from the Tronox Namakwa Sands Mine at Brand-se-Baai in the Northern Cape province of South Africa. Methyl orange powder (85 %), sulphuric acid (H_2SO_4) (98 %) and H_2O_2 (30 %) were all purchased from Sigma Aldrich. All materials were used as received without further processing, apart from H_2SO_4, which was diluted with ultrapure (de-ionised) water before use. De-ionised water from a Purelab Flex 3 was used in the mixing of all solutions.

3.2 Catalyst Characterisation

Catalyst characterisation was performed on the ilmenite sample to determine the properties of the material. The catalyst sample was chosen as it was predominantly ilmenite. However, natural and non-refined sands are presumed to contain impurities. The ilmenite was analysed in terms of mineralogy, chemical composition, morphology and Brunauer-Emmett-Teller (BET) surface area. The characterisation indicates the potential catalytic activity of the material. The findings were used as a baseline for comparisons with other studies to determine whether physical or chemical change occurred to the catalyst after recovering from the degradation process.

3.2.1 X-ray Diffraction (XRD)

The mineralogy of the ilmenite catalyst was determined through X-Ray Diffraction (XRD) analysis. The samples were prepared according to the standardised Panalytical backloading system, which randomly distributes the particles. The analysis was conducted using the PANalytical X'Pert Pro powder diffractometer in θ-θ configuration with an X'Celerator detector and variable divergence with Fe filtered Co-Kα radiation (λ = 1.789 Å) fixed slits. Mineral phases were determined using X'Pert Highscore plus software by selecting the best-fitting pattern from the ICSD database. The relative phase weight percentage was estimated using the Rietveld method.

3.2.2 X-ray Fluorescence (XRF)

The elemental composition of the catalyst was determined through X-Ray Fluorescence (XRF) analysis. The samples were prepared as pressed powders where a 10 – 30 g powered sample was mixed with 20 drops of Moviol (PVA) and then pressed to 10 tonnes. The analysis was conducted using the Thermo Fisher ARL Perform'X Sequential XRF instrument with Uniquant software. Only elements found above the detection limits were reported. The values were normalised, as no loss on ignition (LOI) was performed. Standard sample material was prepared and analysed in the same way as the samples and is reported as such.

3.2.3 Scanning Electron Microscopy (SEM-EDS)

The morphology and elemental distribution of the sample were analysed using a Zeiss Ultra PLUS FEG SEM using the Oxford instruments detector and Aztec 3.0 software SP1. The samples were placed on pieces of carbon tape that were attached to an aluminium plate. The plate with the samples was then carbon coated three times using an SEM auto-coating unit E2500 (Polaron Equipment Ltd) sputter coater. These samples were used to determine the morphology of the particles that make up the catalyst material.

Separate samples were prepared to analyse the elemental distribution of the material. These samples were embedded in epoxy resin and left to polymerize overnight in an oven at 60 °C. The samples were polished using four different sandpaper grades (180, 360, 1200, 2400), starting with the lowest and moving to the highest grades. Following polishing, this sample was also carbon coated.

3.2.4 Brunauer-Emmett-Teller (BET) Surface Area

BET surface area analysis was conducted using a Quantachrome (NOVAtouch NT 2LX-1) driven by TouchWin Software Version 1.22. To determine texture, the sample was loaded into a quartz tube for degassing at 80 °C before the nitrogen adsorption-desorption test. The specific surface area data was obtained using the Brunauer-Emmett-Teller (BET) model.

28

3.3 Degradation Studies

A photoreactor was set up to create the conditions for the Fenton-like reaction. Methyl orange was chosen as the target pollutant in this study due to its phenolic nature, which means it is highly stable and resistant to conventional wastewater treatment. Initial conditions of operation were chosen based on what previous literature has found to be optimal.

3.3.1 Foundational Experiment

Experiments were conducted following a standard procedure and setup (**Figure 4**). A 400 ml solution of 10 mg/L methyl orange (pH adjusted to 3) was placed in the dark on a magnetic stirrer in a temperature control room (20 °C). To this, 1000 mg/L (400 mg) of ilmenite was added, and the solution was left to equilibrate in the dark for 30 minutes (T = -30 min). A 2.5 mM dose of H_2O_2 was added to activate the reaction (T = 0 min). Samples were taken at regular time intervals, centrifuged and the supernatant collected. All experiments were performed in duplicate at the same time to allow for the best comparison. Methyl orange concentrations were determined using a spectrophotometer (WPA-Lightwave II) at a wavelength of 503 nm.

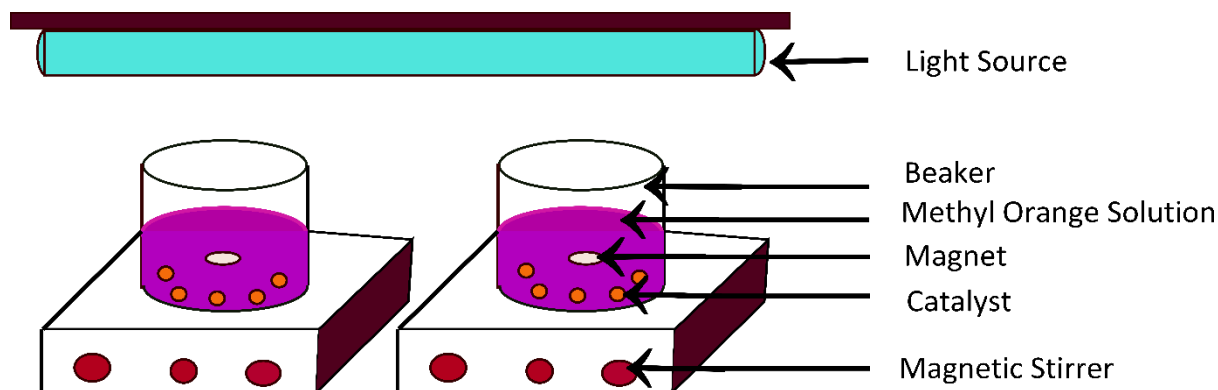**Figure 4:**   Experimental Setup for degradation studies

The experimental setup seen in **Figure 4** was placed inside an enclosed chamber covered with reflective material. A tubular globe fitting was attached on the roof of the chamber for photo-Fenton experiments conducted later on in the optimisation processes. These conditions were chosen as the starting points from which the optimisation experiments were built.

3.3.2 Impact on Catalyst

A batch experiment was conducted at a magnitude of 5 times the original. This experiment was run for 24 hours, after which the catalyst mass was recovered. The catalyst was rinsed with 200 ml of 0.1 M KCl solution to remove any amorphous material sorbed to the surface. The catalyst was then rinsed twice with de-ionised water and left to dry before XRD and XRF analysis.

3.4 Process optimisation of affecting variables

All degradation experiments were conducted using the setup displayed in **Figure 4**. The Initial conditions used were the same as the initial experiment, with changes made to the concentrations or levels of the parameter being optimised. Firstly, pH and irradiation optimisations were performed. Three different pH levels (2.0, 2.5, 3.0, 5.0) were tested against four different irradiation sources (Dark, UVA, UVB, Visible) in a total of twelve experiments of a fractional factorial design. The model, make, and wavelength of the different lamps used are listed in **Table 2**. Catalyst loading was optimised next using the optimal pH and irradiation found in the previous experiment. Catalyst loading was done in a range from 0 mg/L to 2500 mg/L in increments of 250 mg/L. Lastly, the H_2O_2 dose was optimised, starting at 0.0 mM to 40 mM.

Table 2: The model and peak wavelengths of the different lamps used for irradiation (Butt and Tichapondwa, 2020)

Irradiation Type	Model	Peak Wavelengths (nm)
UVA	Philips TL-K 40W/10R Actinic BL Reflector	365
UVB	Exo Terra Reptile UVB 200 18W, 60 cm	310 – 350
Visible	Philips Master Super 80 TL-D 18W/865	440, 560, 640

Once optimal conditions were determined, methyl orange concentrations were varied. Experiments were conducted at optimal conditions with concentrations of methyl orange at 5 mg/L, 10 mg/L and 20 mg/L. These results were also used to model the kinetics of the reaction.

3.4.1.1   Iron Leaching

Iron leaching tests were conducted in conjunction with pH optimisation (2.0, 2.5, 3.0, 5.0) and catalyst loading optimisation (0 mg/L – 2500 mg/L) to help determine the role of iron in the reaction. The samples were analysed using the Spectro Genesis Inductively Coupled Plasma Optical Emission Spectrometry (ICP-OES).

3.5   Analytical Methods

Analytical methods were employed to determine the extent of degradation and the degree of mineralisation of the methyl orange under optimal operating conditions.

3.5.1   Liquid chromatography Mass Spectrometry (LC-MS)

Liquid Chromatography-Mass Spectrometry (LC-MS) was performed on samples before that addition of catalyst and H_2O_2, and a sample was collected 60 minutes after the reaction started. The samples were analysed for the presence of methyl orange following the reaction. The samples were analysed using a Nexera LC-40 System coupled to an LCMS-9030 Q-TOF operated in negative ESI mode. Chromatographic separation was performed using a gradient of mobile phase (A), water containing 0.1 % (v/v) formic acid, and (B) acetonitrile.

A calibration curve was established using a five-point calibration from 0.1 μg/mL to 10 μg/mL methyl orange.

3.5.2   Total Organic Carbon (TOC)

The degree of mineralisation was determined by analysing the Total Organic Carbon (TOC). TOC is the percentage of organic carbon in a solution and therefore can indicate the concentration of organic pollutants in the solution. The endpoint of the mineralisation of an organic compound is the formation of H_2O and CO_2 gas. As this mineralisation process occurs, the TOC content in the solution should decrease with organic carbon being converted into CO_2. Experiments were conducted at optimal operating conditions. A 40 ml sample was taken before the activation of the reaction and after 60 minutes of reaction. The sample was filtered into a TOC vial for analysis using the SHIMADZU TOC-V wp instrument.

4 CHAPTER FOUR: CATALYST CHARACTERISATION

The chemical and physical properties of the raw catalyst were determined through various methods. The characterisation was done to help understand the chemical processes at work during the degradation reactions. The catalysts mineralogy was determined by X-Ray Diffraction (XRD), its morphological characteristics by Scanning Electron Microscopy (SEM) and its elemental composition by X-Ray Fluorescence (XRF) and SEM- Energy Dispersive X-ray Spectroscopy (EDS). The catalyst surface area was determined by BET Surface Area analysis.

4.1 XRD

XRD analysis was used to determine the mineral phases and their percentage contribution of the catalyst samples. Two samples were analysed, the raw catalyst and the catalyst recovered from the initial degradation experiment, run at five times the quantity.

The most pronounced peaks ($2\theta = 27.8°$, $38.1°$, $41.2°$ and $62.5°$) on the diffractogram (**Figure 5**) were found to correspond to ilmenite, along with several other minor peaks. Ilmenite made up the bulk of the catalyst sample at 83.5 wt. %. Hematite was the second most dominant mineral at approximately 15 wt. %. Hematite (Fe_2O_3) is a common iron oxide found in soil; it comprises mainly iron in Fe (III). Hematite can behave as an effective catalyst in AOPs under the right conditions and thus contribute to the performance of the raw ilmenite sample (Munoz et al., 2017). The overall mineralogy of the catalyst used is detailed in **Table 3**.
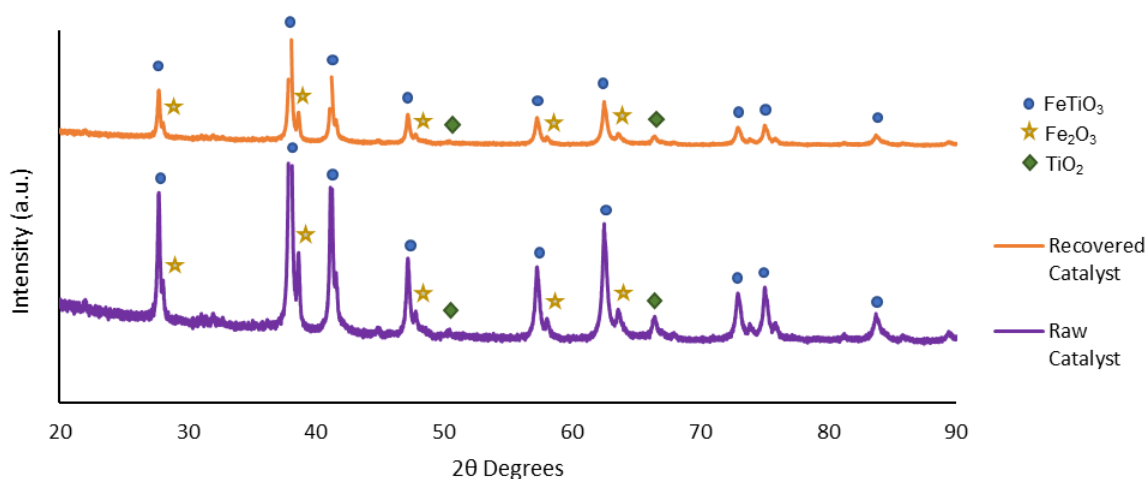
Figure 5:   The XRD (Co-Kα radiation) spectra of raw ilmenite and recovered ilmenite after degradation

The sample contains a low percentage of rutile, a naturally occurring mineral phase of titanium dioxide (TiO_2). TiO_2 is one of the most widely used catalysts in photocatalysis due to its ability to generate electron/hole pairs under the influence of light. When the light of a specific wavelength hits the photocatalyst, an electron gets excited and moves from the valence band to the conduction band, creating a hole (h^+) which acts as an oxidising agent and can thus break down organic compounds (Ameta et al., 2018b).

Table 3:   The mineral composition of the raw and recovered catalyst in weight percentage as determined through XRD analysis

Mineral Phase	Mineral Composition	Raw catalyst (wt. %)	Recovered catalyst (wt. %)
Ilmenite	$FeTiO_3$	83.53	82.43
Hematite	Fe_2O_3	14.99	16.08
Rutile	TiO_2	1.2	1.49
Quartz	SiO_2	0.28	-

33

A study conducted by Tichapondwa et al. (2020) compared the photocatalytic effect of different TiO_2 mineral phases (rutile, anatase and Degussa P25). The study found that rutile, although comprising of TiO_2, displayed negligible photocatalytic activity, with Degussa P25 recording the highest photocatalytic activity. The presence of rutile in the ilmenite sample are unlikely to contribute to its catalytic activity due to their relatively low concentrations. On the other hand, the sample has a comparatively higher percentage of hematite. Hematite is another iron oxide found abundantly in nature and used in similar studies as a natural catalyst in AOPs. One such study was conducted by Munoz et al. (2017) that examined different iron oxides as natural catalysts for the CWPO process using phenol as a pollutant. The study found that hematite showed a better TOC conversion than ilmenite and that both minerals displayed low iron leaching. Therefore, the presence of a large percentage of hematite in this sample might positively contribute to its catalytic activity.

The overall mineral phase composition of the raw and recovered catalyst is very similar, with slight changes in percentage weight contribution, as shown in **Table 3**. The slight changes in the composition of the raw and recovered catalyst can be attributed to uneven sampling and particle distribution.

4.2 XRF

XRF was conducted to determine the elemental composition of the catalyst. The analysis showed that iron and titanium comprise the most significant weight percentages of the ilmenite sample. **Table 4** presents the elemental composition of the catalyst in weight percentage as determined by XRF. Refer to **Appendix A** for the full XRF report.

Table 4: The elemental composition of the raw ilmenite catalyst as weight percentage determined through XRF

Element	Weight Percentage (wt. %)
Iron (Fe)	34.60
Titanium (Ti)	32.30

*Oxygen (O)	28.73
**Trace Elements (Mn, Si, Al, Mg, V, Cr and K)	4.37

* Calculated

**Listed in descending order of weight percentage

The high percentages of Fe and Ti are due to the majority of the sample being made up of ilmenite, as seen in the XRD analysis. The theoretical weight percentages of pure ilmenite are 36.8 % Fe, 31.6 % Ti and 31.6 % O; however, since the present sample is natural and not purified, it is expected that there will be variations and an expected amount of substitution by other trace elements (Klein and Dutrow, 2007).

Trace elements such as manganese (Mn), magnesium (Mg), aluminium (Al) and vanadium (V) were detected in the sample at weight percentages of 0.95, 0.72, 0.62 and 0.22, respectively. Such impurities are expected in naturally occurring minerals as Mn, Mg, Al, and V are common elements that occur through isomorphic substitution in minerals that have been subject to weathering (Klein and Dutrow, 2007).

4.3 Scanning Electron Microscopy-Energy Dispersive X-Ray Spectroscopy (SEM-EDS)

SEM was employed to determine the morphology and SEM-EDS was used to determine the elemental composition and dispersion.

4.3.1 Morphology

An unpolished sample of the raw catalyst was analysed through SEM imaging to determine the shape and size of the individual particles. **Figure 6** shows the morphology and size of the particles in the catalyst.
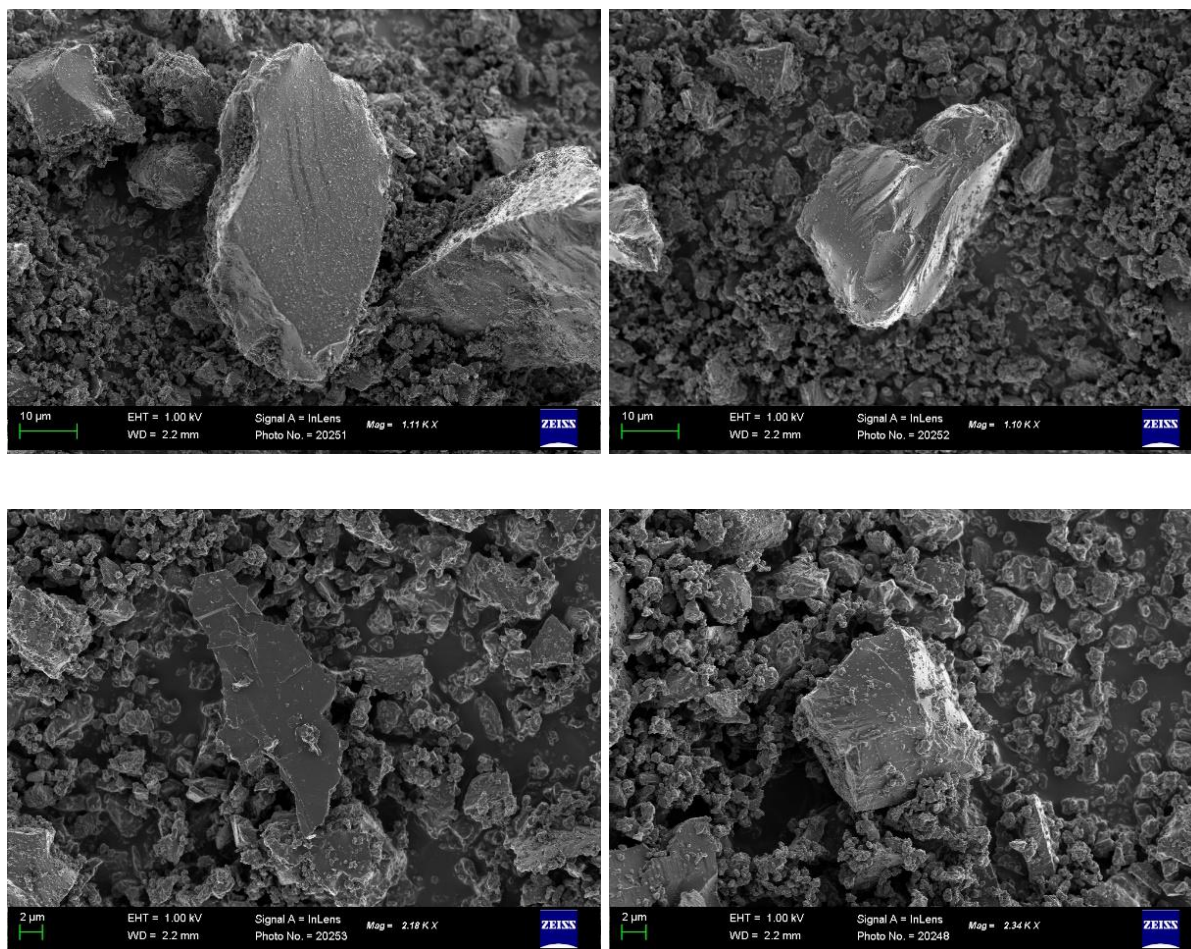
Figure 6:   Particle morphological images of the catalyst sample

The larger particles had angular and irregular shapes, whilst the smaller particles were granular. Most of the larger particles identified were between 5 μm and 30 μm in size. The sample contained many smaller sized particles of a granular or crumb, rounded shape. Due to the large size of the particles, it is postulated that adsorption will be negligible.

4.3.2   Elemental Distribution

The micrographs obtained from SEM-EDS (**Figure 7**) show a relatively even distribution of iron and titanium over the sample space indicative of ilmenite. Small areas of silicon can also be seen, which can be attributed to the presence of quartz minerals. The SEM micrographs support the XRD and XRF analysis findings with the large majority of the particles containing titanium and iron; this indicates ilmenite, and the XRD detected hematite and rutile.
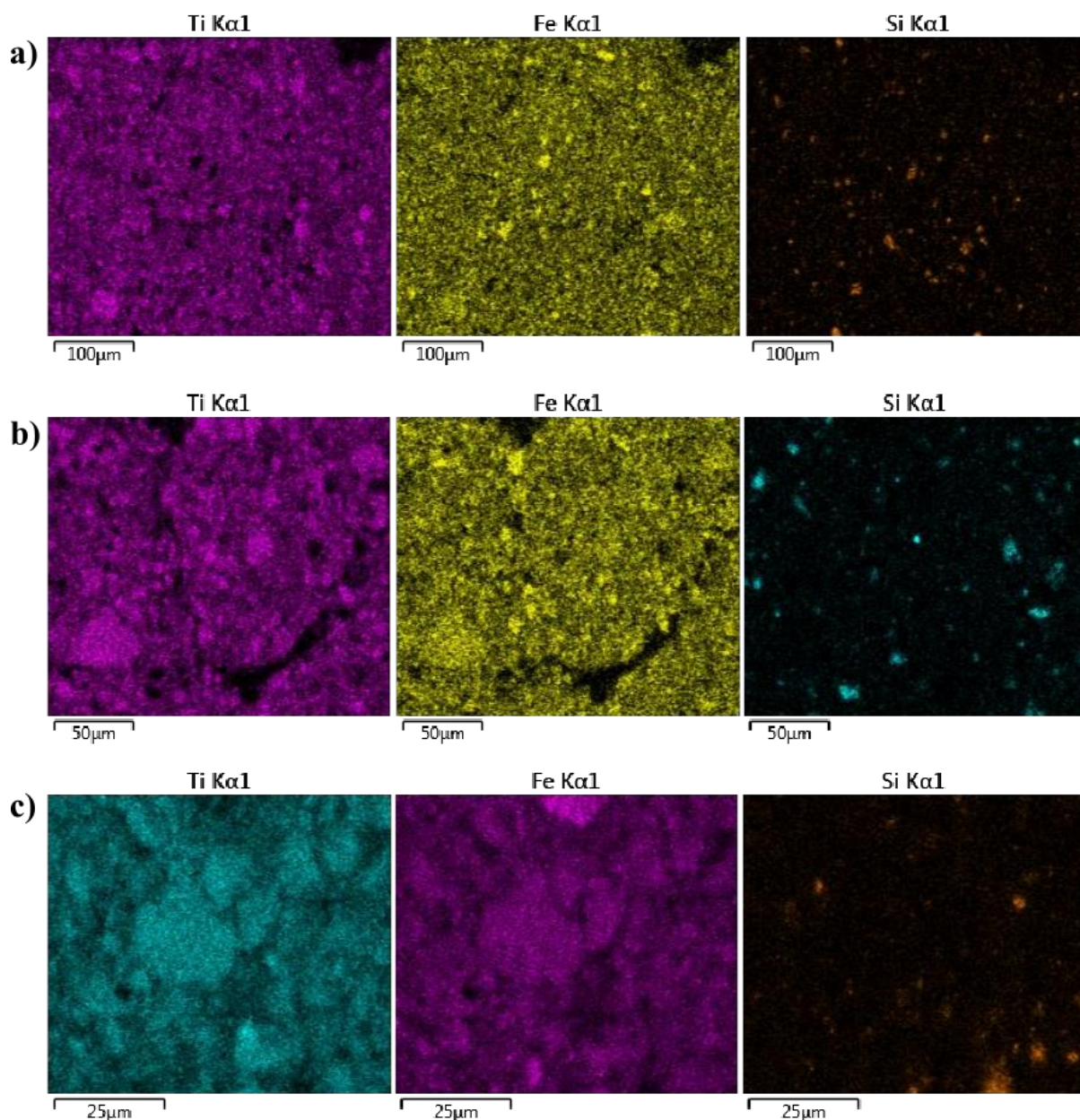
Figure 7:   SEM-EDS Micrographs of three different sites (a, b and c) of the catalyst sample using EDS to determine the elemental composition

4.4 BET Surface Area & Pore Size Distribution

The isotherm from nitrogen adsorption-desorption BET analysis showed a curve (**Figure 8**) representing a low adsorption capacity (Yurdakal et al., 2019). The adsorption-desorption graph is a type III graph meaning that absorption increases exponentially with an increase in pressure, indicating weak interaction (Hattori and Kaneko, 2013). The BET surface area for the catalyst sample was found to be 10.42 m^2/g, which is considered to be a low BET surface

37

area although slightly higher than the ilmenite used in other studies, which lies between 4 and 6 m^2/g (García-Muñoz et al., 2016a, Pataquiva-Mateus et al., 2017, Silveira et al., 2017). It was postulated that the smaller crumb structured particles seen in the SEM-EDS images (**Figure 6**) gave rise to this higher BET. Half pore width was measured to be between 1 nm and 10 nm indicating the presence of micropores ($<$ 2 nm) and mesopores (2-50 nm). The low BET surface area suggests that the catalyst will present low adsorption abilities.

Figure 8: The BET adsorption-desorption isotherm of the catalyst sample

4.5 Comparison with Ilmenite in other Studies

The XRD, XRF and BET surface area data from the ilmenite catalyst in this study was also published by Butt and Tichapondwa (2020), compared to the ilmenite catalysts used in this study other similar studies. **Table 5** displays the results comparatively.

38
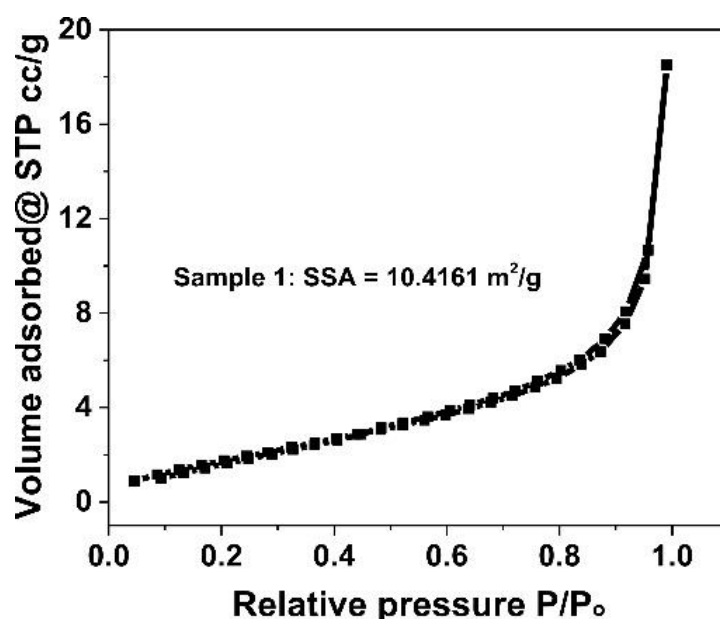
Table 5: Comparison of the ilmenite catalyst used in this study to the ilmenite used in other studies

Study	XRD (%)			XRF (%)		BET (m²/g)
	$FeTiO_3$	Fe_2O_3	TiO_2	Fe	Ti	
Butt and Tichapondwa (2020) (Present Study)	83.53	14.99	1.2	34.60	32.30	10.42
Recovered Catalyst (Present Study)	82.43	16.08	1.49	-	-	-
García-Muñoz et al. (2016a)	85	-	15	36	37	6
Canas-Martinez et al. (2019)	69.50	2.81	4.18	NA*	NA*	NA*
Silveira et al. (2017)	85	-	15	36	37	6
Munoz et al. (2017)	NA*	NA*	NA*	36.2	37.0	4

* Information not given in paper

This study reported lower titanium and iron content compared to previous studies. This can be due to other trace elements found in the sample that were not present in the other authors' ilmenite due to the purification of the ilmenite they used. The other three studies whose ilmenite data was used for comparison displayed higher titanium and iron contents (**Table 5**). Their samples were very similar, with no presence of hematite and higher percentages of ilmenite and rutile. It is expected that the sample in this study will display a much lower photocatalytic activity than the ones in the above sample due to the low percentage of titanium dioxide in the sample.

The sample in this study had a higher BET surface area than any of the other studies. This indicates that the sample is likely to have a more considerable absorbance potential, although not by much.

4.6 Summary

The ilmenite catalyst was characterised by using XRD, XRF and BET surface area. The catalyst was found to have 83.53 % $FeTiO_3$, 14.99 % Fe_2O_3 and 1.2 % TiO_2, with a total Fe of 34.60 % and Ti of 32.30 %. The catalyst is mainly comprised of ilmenite and partially of hematite. This sample does contain rutile but in a much lower quantity than seen in the other studies. This indicates that the catalyst is likely to have low photocatalytic potential. However, the high iron content and presence of hematite indicate that the catalyst should be effective in a Fenton-like Reaction. The catalyst has a low BET surface area of 10.42 m^2/g; although this is higher than most comparative studies, minimal absorption is expected.

5 CHAPTER FIVE: DEGRADATION STUDIES

5.1 Introduction

The main aim of this research was to determine whether naturally-occurring, South African Ilmenite could be a suitable and effective catalyst for the degradation of organic pollutants in a Fenton-like reaction.

5.1.1 Foundational Experiments

Figure 9 shows the decolourisation of methyl orange over time in the absence and presence of various parameters operating. Partial decolourisation occurred in the presence of ilmenite and H_2O_2, indicating that degradation was occurring. These results show the system behaves similarly to the classic Fenton's Reaction, whereby the "iron salt" and H_2O_2 are needed for the reaction to occur.
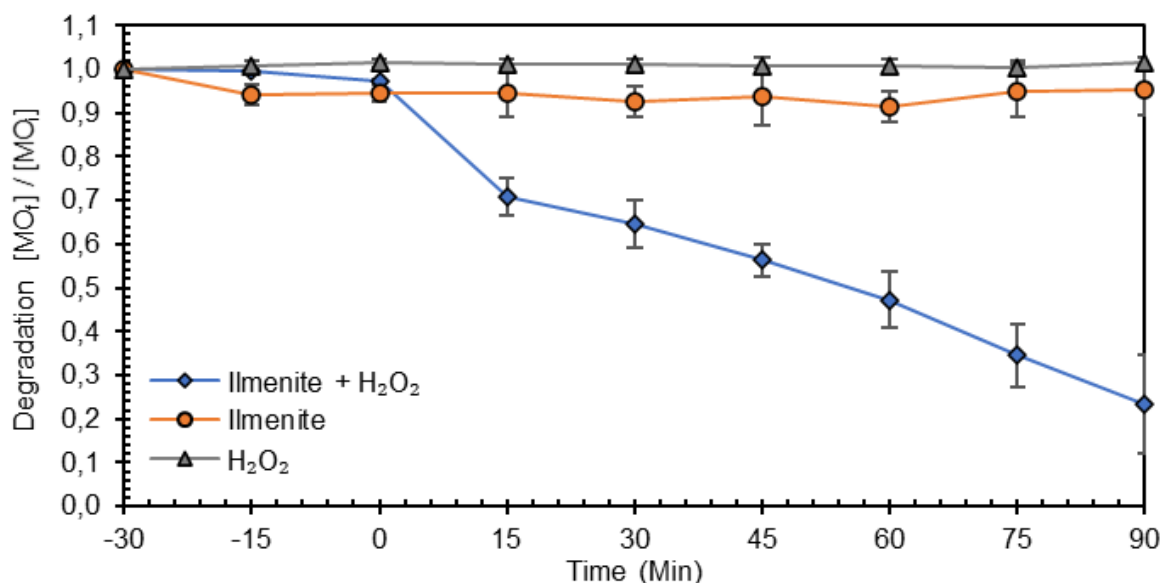
Figure 9: The degradation of methyl orange under the presence and/or absence of various parameters. Operating conditions: [MO] = 10 mg/L, [H_2O_2] = 2.5 mM, [Ilmenite] = 1000 mg/L, pH = 3.0, Temperature = ± 20 °C

The slight degradation observed in the presence of ilmenite only can be attributed to absorption by the surface; however, this constitutes a degradation below 10 %. The low absorption can be due to the low BET surface area (Yurdakal et al., 2019). No noticeable degradation was

41

observed in the absence of ilmenite which suggests that the H_2O_2 is not decomposing into •OH radicals but rather H_2O and O_2, however the chemistry of H_2O_2 decomposition is still not fully understood (Barbusinski, 2009). This is expected as H_2O_2 is more stable at low pH values and will only induce a redox reaction in the presence of a redox-active ion and an organic substrate (Kuo, 1992). These results imply that interaction is required between the ilmenite and the H_2O_2 to generate the free radicals required to degrade the methyl orange molecules. Therefore, it is assumed that the reaction follows a similar mechanism to that of the Heterogeneous Fenton reaction, whereby Fe (III) on the catalyst surface undergoes reduction to Fe (II) due to the low pH. Iron oxides are sparsely soluble under neutral pH levels, and solubility increases with a more acidic pH (Cornell and Schwertmann, 2003).

5.2   Process optimisation

Process optimisation experiments were conducted between irradiation and pH; then, the system was optimised for catalyst loading and H_2O_2 dose. Lastly, experiments were conducted at optimal operating conditions with changes to the methyl orange concentration to determine if the methyl orange concentration impacted the degradation rate.

5.2.1   Effect of pH and Light

The pH has a critical role in the Fenton's reaction. The optimal pH associated with the classic Fenton Reaction is reportedly between two and three. **Figure 10** shows the degradation of methyl orange at different pH levels (2.0, 2.5, 3.0) under different light sources (Dark, UVA, UVB, Visible). It is seen that the fastest degradation occurs in the presence of UVB irradiation at all pH levels, with complete decolourisation occurring after 90, 60 and 75 minutes for the pH levels 2.0, 2.5 and 3.0, respectively.
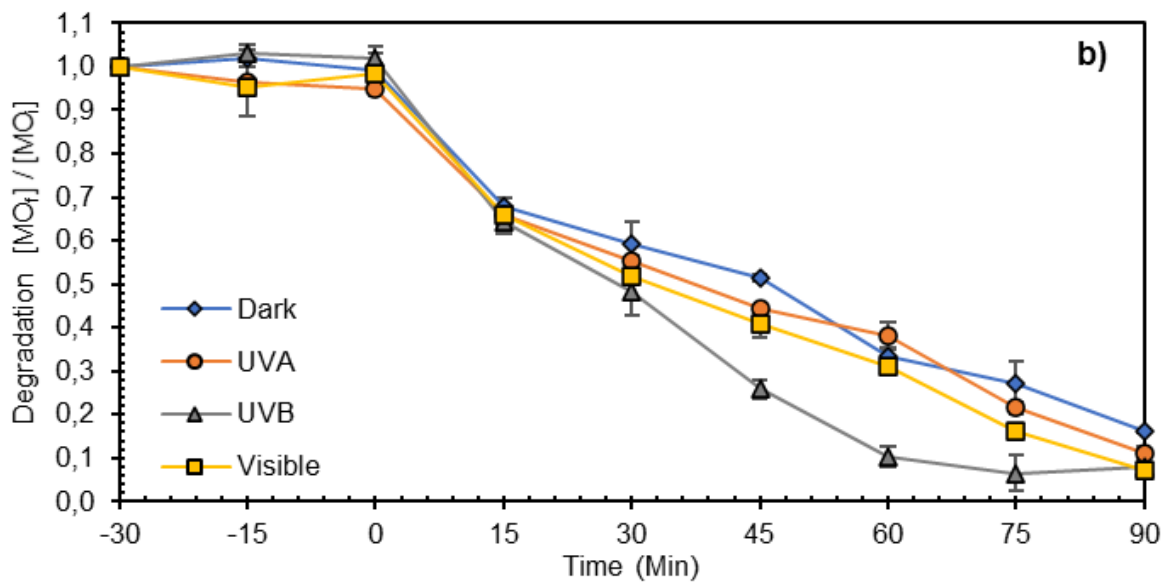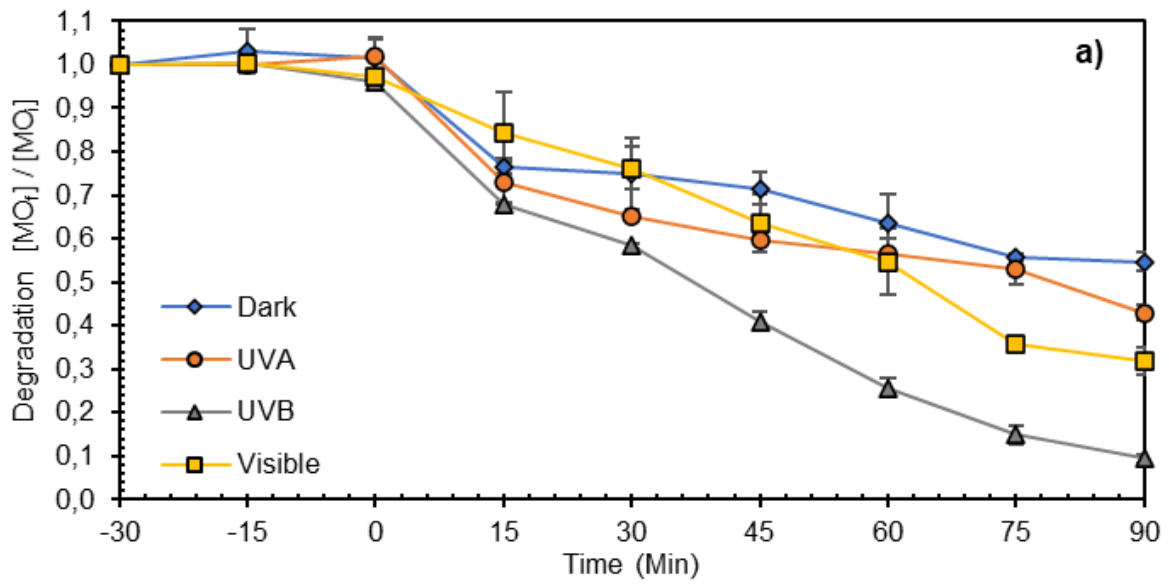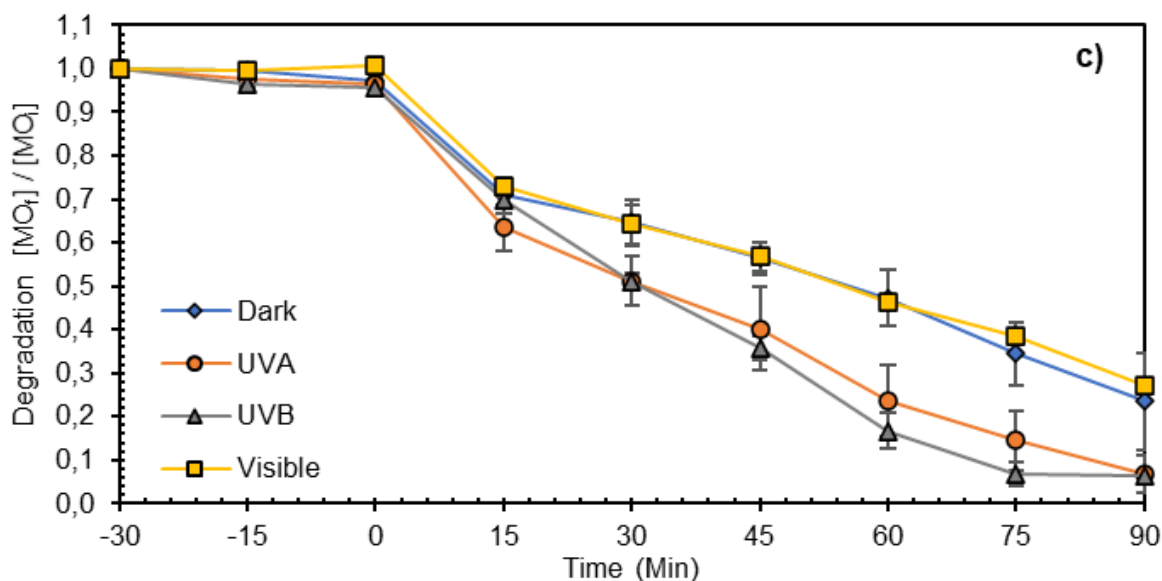
Figure 10: The influence of pH and irradiation on the degradation rates of methyl orange (a. pH 2.0, b. pH 2.5, c. pH 3.0). Operating conditions: [MO] = 10 mg/L, $[H_2O_2]$ = 2.5 mM, [Ilmenite] = 1000 mg/L, Temperature = ± 20 °C

The present results are supported by literature that claims that UVB irradiation is the most effective for Fe^{3+} photoreduction, thus increasing the amount of Fe^{2+} in the system compared to other irradiation wavelengths (Rijkenberg et al., 2004, Rijkenberg et al., 2005, Lueder et al., 2020). A study by Rijkenberg et al. (2005) sought to investigate the effect of different irradiation types (UVA, UVB and Visible) on the photoreduction of iron. The study concluded that UVB led to the highest concentration of Fe^{2+} compared to UVA and visible irradiation; the authors postulated that there were two possible reasons for this: (1) the concentration of radioisotopic iron was higher under UVB irradiation leading to a higher concentration of photoreactive iron or (2) the Colour Dissolved Organic Matter (CDOM) concentration was higher in the experiment using UVB irradiation. The second reason suggests that dissolved organic matter may impact the cycling of iron in terms of producing superoxides which cause the reduction of iron.

A study conducted by Eskandarian et al. (2016) on the degradation of pharmaceuticals using TiO_2 in photocatalysis examined the effect of different wavelengths on degradation efficiency. The study found that as irradiation wavelength increased, photo energy decreased and thus, degradation rates also decreased. This could be one of the reasons that UVB irradiation was found to have a faster degradation rate compared to UVA and visible light wavelengths.

UV irradiation is also influenced by the intensity (wattage) and the distance from the solution (Sajjad and Al-zobai, 2020). A study conducted by Sajjad and Al-zobai (2020) investigated the effect of light intensity, distance and direction on the efficacy of the photo-Fenton reaction using reactive blue dye as the pollutant. The study found that a light intensity of 24 W at a distance of 15 cm provided the fastest degradation rate; this can explain the lower impact of the present results as a light intensity of 18 W was also used at approximately 15 cm.

The influence of pH on the degradation rate of methyl orange in the presence of UVB irradiation is displayed graphically in **Figure 11a** alongside the iron leaching concentrations at the same pH levels. These experiments were conducted to determine which pH was optimal under UVB irradiation.
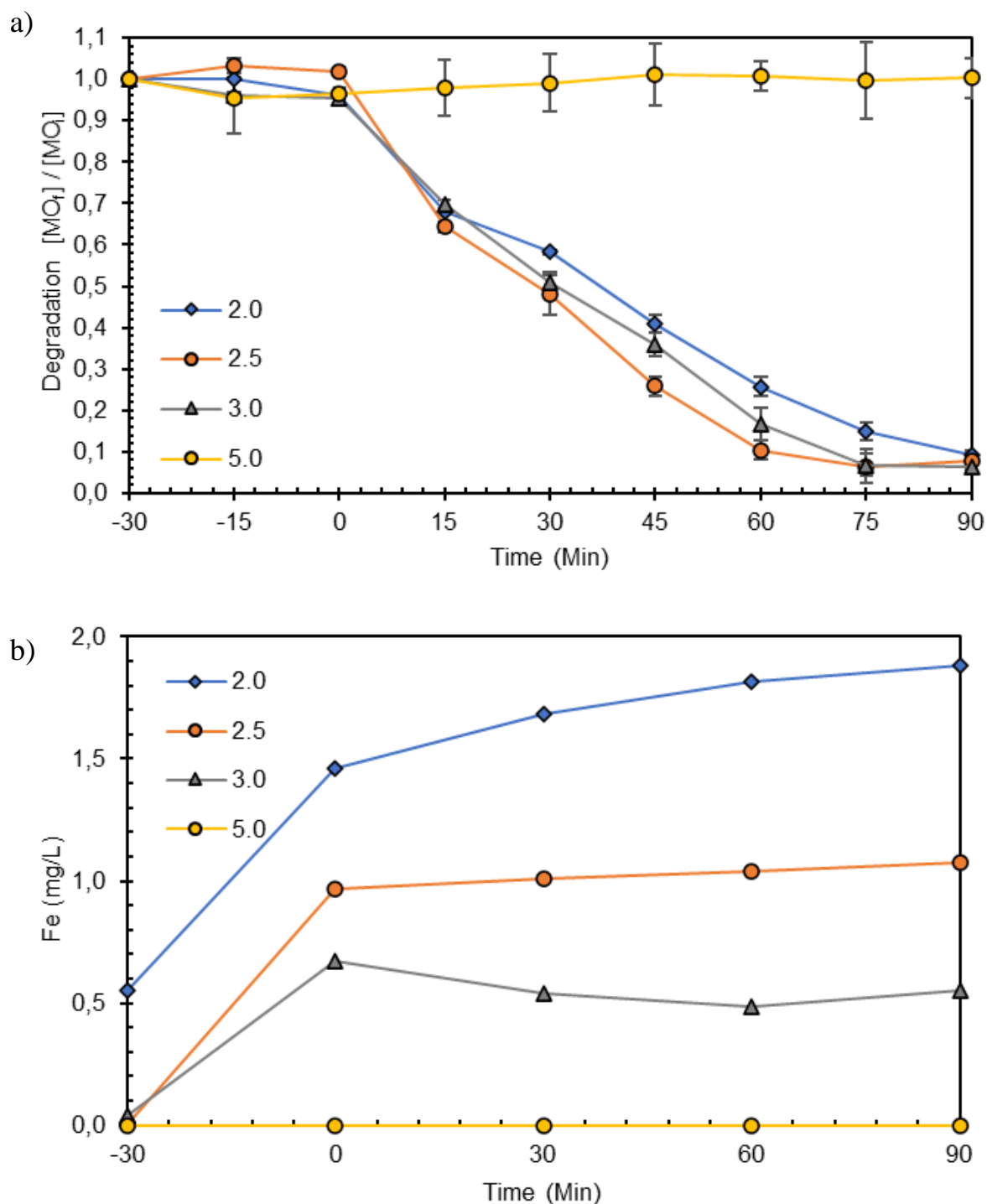
a)

b)

Figure 11: a) The degradation of methyl orange at different pH levels under the influence of UVB irradiation; b) The iron concentration at different pH levels under the influence of UVB. Operating conditions: [MO] = 10 mg/L, $[H_2O_2]$ = 2.5 mM, [Ilmenite] = 1000 mg/L, Temperature = ± 20 °C, Irradiation = UVB (λ = 310 – 350 nm)

A pH value of 2.5 was found to be optimal under the influence of UVB irradiation. This is explained through the behaviour of Fe and H_2O_2 at different pH values. At pH values above 3.0, the reduced iron could re-oxidise and precipitate, thus decreasing the generation of •OH; on the other hand, a pH value below 2.5 could increase the scavenging effect of •OH by excess generated H^+ (Wang et al., 2016). The scavenging effect serves to explains why a pH of 2.5 was found to be optimal. García-Muñoz et al. (2018) showed that the use of ilmenite in the CWPO process could work efficiently at a circumneutral pH; this can be due to the high percentage of rutile in the authors ilmenite sample. The authors suggest that different mechanisms drive H_2O_2 decomposition under different pH levels and that under a circumneutral pH, the decomposition of H_2O_2 is driven mainly through the generation of electron/hole pairs that can be attributed to the TiO_2 content. Since the catalyst used in this study has negligible TiO_2 content is unsurprising that no degradation was observed at a pH level of 5.0. This is further supported by the iron leaching results in **Figure 11b**.

As the pH increases from 2.0 to 3.0, there is a decrease in iron in the solution; however, no iron leaching occurred at neutral pH levels (5.0). These results indicate that aqueous iron is necessary for the degradation reactions to occur. This confirms that the primary reaction mechanism follows that of the classic Fenton reagent. Firstly, Fe (II) enters the solution through protonation driven dissolution caused by the low pH (reaction 10) (Sparks, 2003b).

$$FeTiO_{3_{(s)}} + 2H^+_{(aq)} \rightarrow FeTiO_{3_{(s)}} + Fe\ (II)_{(aq)} \hspace{3cm} (10)$$
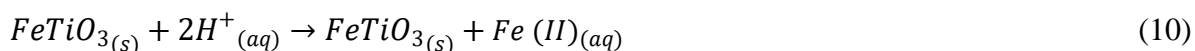
After that, the dissolved Fe ions react with H_2O_2 to produce Fe (III), OH^- and a •OH radical (reaction 11).

$$Fe\ (II)_{(aq)} + H_2O_{2_{(aq)}} \rightarrow Fe\ (III)_{(aq)} + \bullet OH_{(aq)} + OH^-_{(aq)} \hspace{2cm} (11)$$
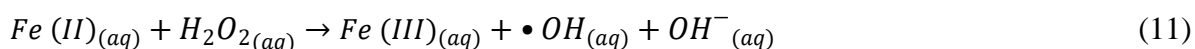
The generated •OH radical reacts with the methyl orange compound, breaking down the azo dye bonds and likely producing short-chain organic acids (reaction 12).

$$C_{14}H_{14}N_3NaS_{(aq)} + \bullet OH_{(aq)} \rightarrow (Short\ Chain\ Organic\ Acids) \hspace{2cm} (12)$$
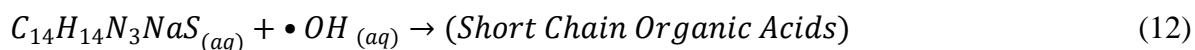
The generated Fe (III) now in solution is reduced by the OH^- to generate more Fe (II) and another •OH radical (reaction 13).

$$Fe\ (III)_{(aq)} + OH^-_{(aq)} \rightarrow Fe\ (II)_{(aq)} + \bullet OH_{(aq)} \hspace{3cm} (13)$$
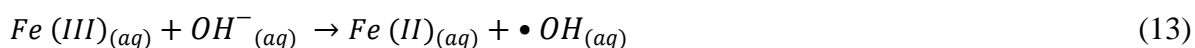
The proposed reaction and iron cycling will continue until the depletion of H_2O_2 in the system.

The pH of the solution affects the speciation of iron in the solution. **Figure 12** is a Pourbaix diagram of pH versus electric potential that graphically displays the relationship between pH and iron speciation.
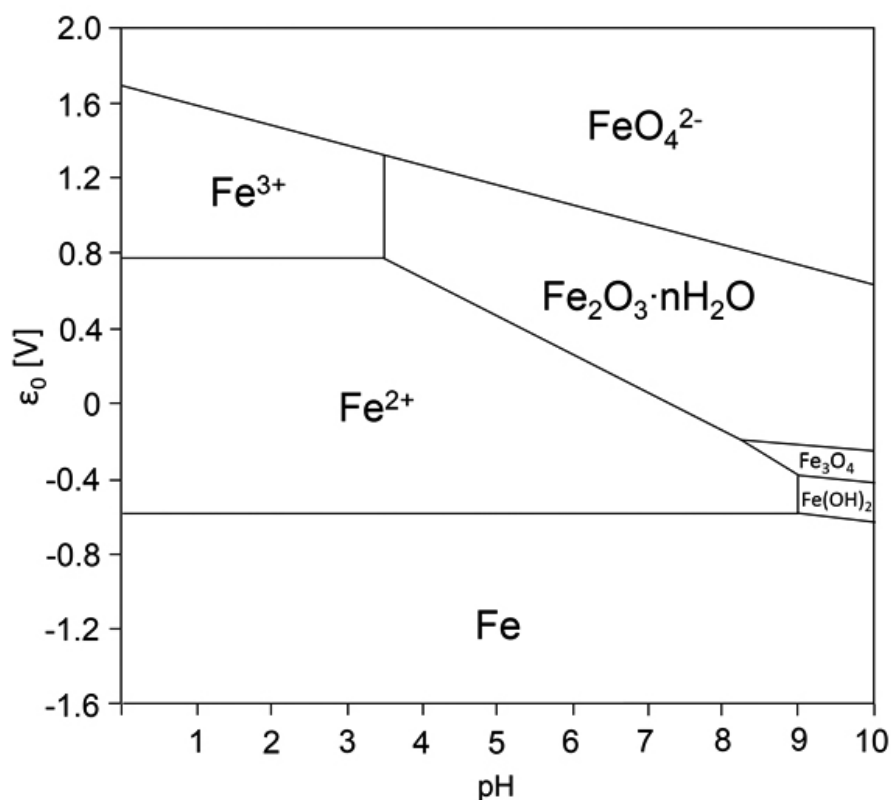
Figure 12: Pourbaix diagram displaying iron species as a function of pH and electronic potential. Taken from publication by Salgado et al. (2013), modified from (Beverskog and Puigdomenech, 1996)

As can be seen, iron speciation differs according to the pH of the solution. At a pH below 9, Fe speciates into Fe (II), and at a pH below four, it speciates into Fe (III). The presence of Fe (III) in solution is necessary for the activation of the Fenton reaction, whereby Fe (III) interacts with H_2O_2 to regenerate Fe (II) ions which in turn react with another molecule of H_2O_2 to generate the $\cdot$OH radicals. This process keeps the cycling of Fe (II) / Fe (III) to allow the system to continually generate the highly oxidative radical $\cdot$OH (Tokumura et al., 2011). The necessity of iron presence in the system also explains why no methyl orange degradation was observed at a pH value of 5.0.

48

Although this process is referred to as a heterogeneous Fenton-like reaction, the mechanism at work occurs largely in the solution. A review article by Nidheesh (2015) discussed the key factors in removing organic pollutants in a heterogeneous Fenton-like system using pyrite (FeS) as a catalyst. Nidheesh (2015) postulated that the most important factor in the catalyst's efficiency was its metal leaching property, specifically the iron leaching property. The author suggested that if a catalyst had a high leaching property, the pollutant degradation would occur in the solution and not on the surface and that the leached iron will undergo a conventional Fenton cycling reaction to form radicals.

5.2.2   Catalyst Loading

The effect of catalyst loading on the MO degradation efficiency was investigated, and it was established that the degradation efficiency increased with increasing catalyst loading (**Figure 13a**). Optimum degradation occurred at a loading of 2000 mg/L; beyond this loading, no appreciable increase was observed. Iron leaching tests were conducted simultaneously with the catalyst loading experiments. **Figure 13b** indicates that catalyst loading was directly proportional to the iron leached in the solution. An increase in catalyst loading leads to an increase in the degradation rate of methyl orange up to 2000 mg/L. An increase in catalyst loading beyond this point did not affect the degradation rate, and thus the optimal catalyst concentration for the degradation of methyl orange is 2000 mg/L. Shorter tests were conducted to determine the iron leaching kinetics (**Figure 13c**).

a)

b)
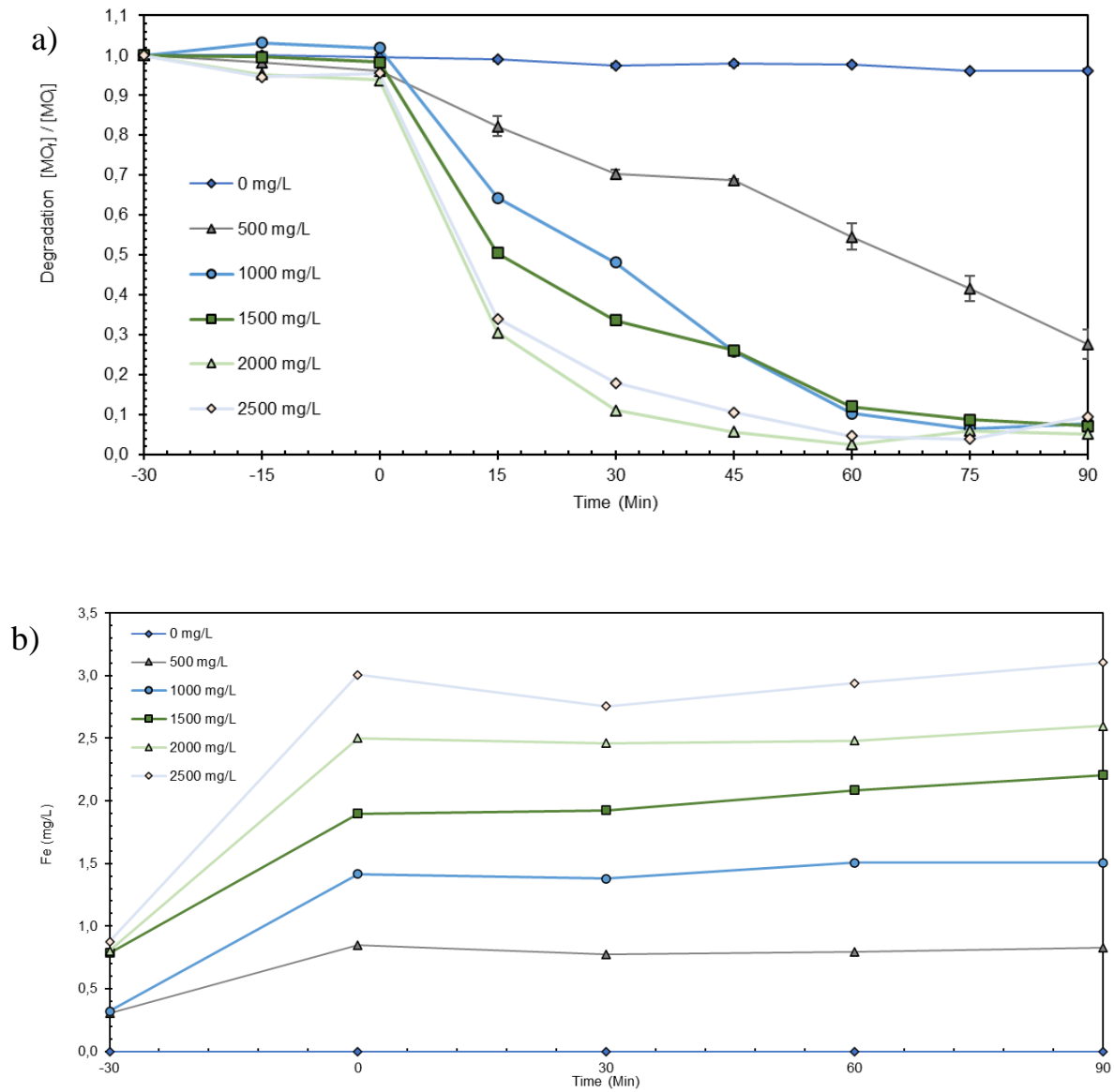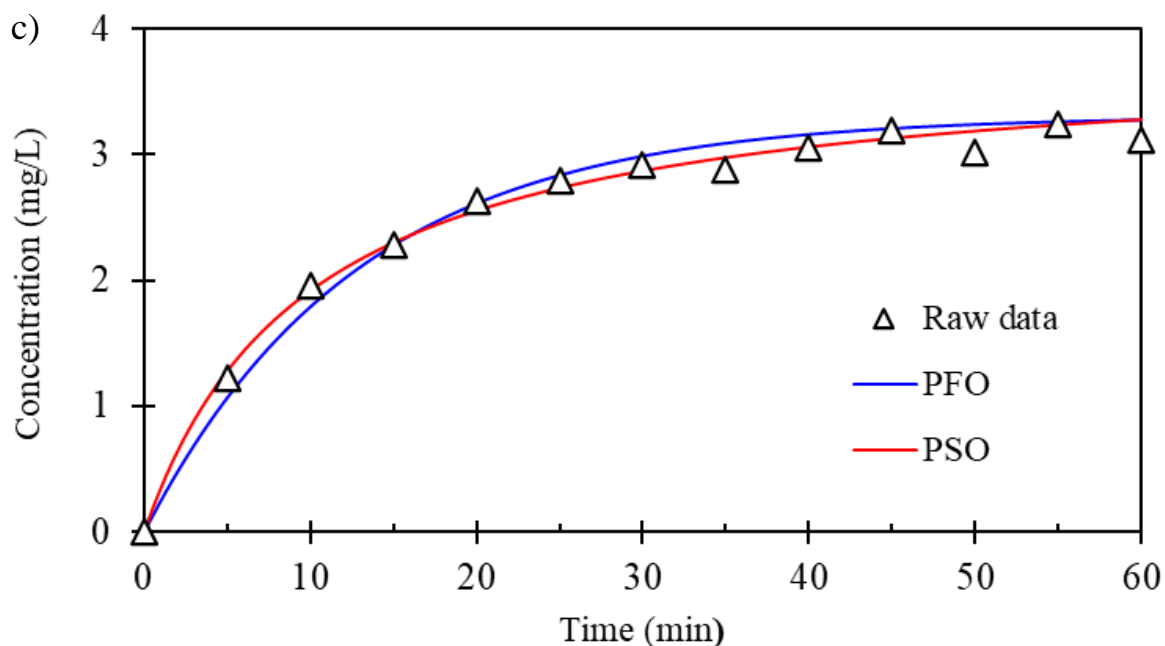
Figure 13: a) The degradation of methyl orange at various catalyst loadings from 0 mg/L – 2500 mg/L; b) the iron concentration at various catalyst loadings over time; c) Pseudo-first and second order kinetics. Operating conditions: [MO] = 10 mg/L, [H_2O_2] = 2.5 mM, pH = 3, Irradiation = UVB (λ = 310 nm – 350 nm), Temperature = $\pm$ 20 °C

No benefit is seen from increasing the catalyst loading past 2000 mg/L; this can be due to the scavenging effect in the excess catalyst (reaction 14, adapted from Wang et al. (2016)).

$$Fe^{2+}{}_{(aq)} + \bullet OH_{(aq)} \rightarrow Fe^{3+}{}_{(aq)} + OH^-{}_{(aq)} \tag{14}$$
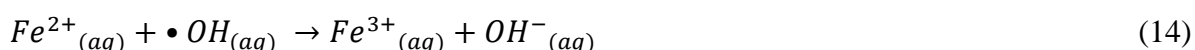
In this reaction, the Fe (II) consumes the OH radical species and thus decreases the reaction rate. Even if excess catalyst does not decrease the reaction rate (as observed above), the excess catalyst will not be utilised appropriately and only increase the cost of operation (Wang et al., 2016).

The amount of Fe (II) leached into the solution at a catalyst loading of 2000 mg/L is greater than that of a pH 2.0, as seen in **Figure 13b**. This implies that the more significant concentration of Fe (II) leached into the solution at a pH of 2.0 did not inhibit the reaction. Rather the reaction was inhibited by the scavenging effect of excess H^+ at a lower pH (Wang et al., 2016). As seen in **Figure 13a**, a catalyst loading above 2000 mg/L has no increased effect on the degradation rate of methyl orange even though slightly more Fe (II) was leached into the solution. This

51

suggests a maximum Fe (II) level in the solution that can react with H_2O_2 to generate •OH radicals. This maximum efficient level of Fe (II) in solution appears to be around 2.6 mg/L. This result is similar to the iron leaching content in a study conducted by García-Muñoz et al. (2016a), which found iron leaching concentrations of 2.3 mg/L. This is particularly interesting as the quantity of ilmenite used in the above study was much less at 450 mg/L. In this work, iron leaching at a similar catalyst loading of 500 mg/L only led to a concentration of ± 0.6 mg/L of Fe in solution.

The rate of degradation appears to be affected by the concentration of Fe (II) in the solution and the pH level of the solution. When the pH is above 2.5, too little Fe (II) is leached into the solution to generate the maximum amount of •OH radicals. However, when the pH is below 2.5, the scavenging effect of excess H^+ on •OH radicals lead to a decrease in the degradation rate even though more Fe (II) is present in the solution.

As seen in **Figure 13c,** kinetics of iron leaching were best predicted by the pseudo-second-order (PSO) model, which had an R^2 value of 0.992 and a rate constant of 0.264 g.mg^{-1}min^{-1} compared to an R^2 of 0.979 and a rate constant 0.78 min^{-1} for the pseudo-first-order (PFO) model. The PSO signifies a better predictor for future work.

5.2.3 H_2O_2 dosage

Figure 14 shows the degradation of methyl orange under different H_2O_2 doses as part of the optimisation process. The optimal H_2O_2 concentration was found to be 1.0 mM. As the H_2O_2 concentration increased, there was an increase in degradation rate up to 1.0 mM; after that, an increase in concentration led to a decrease in degradation rates.
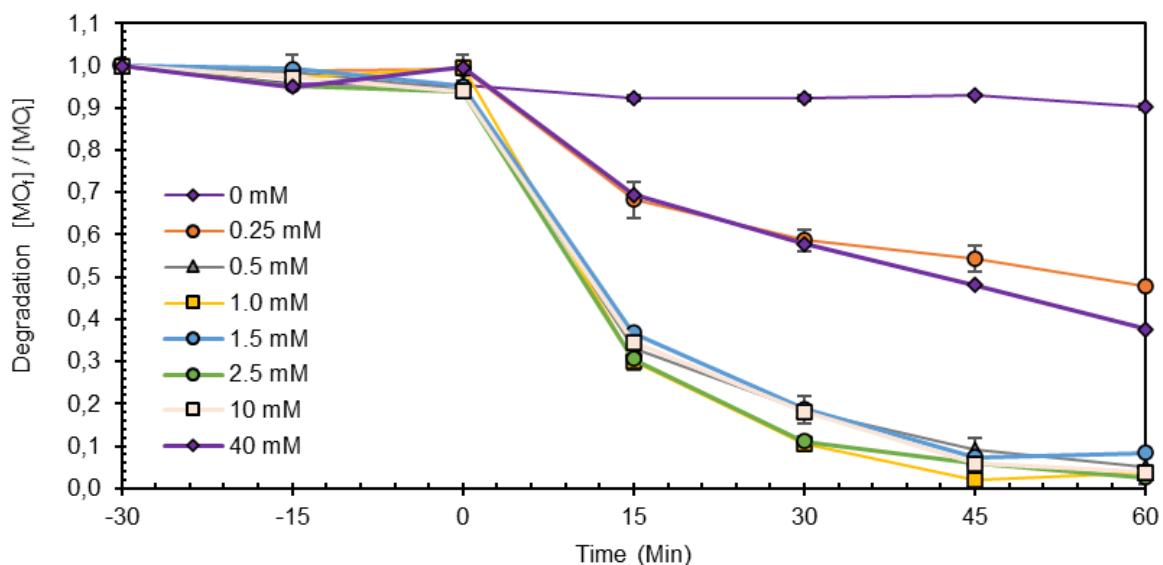
Figure 14: The rate of degradation of methyl orange over time at different H_2O_2 doses. Operating conditions: $[MO] = 10$ mg/L, $[Ilmenite] = 2000$ mg/L, pH = 3, Irradiation = UVB ($\lambda = 310$ nm – 350 nm), Temperature = $\pm$ 20 °C

As the H_2O_2 concentration increased, there was an increase in degradation rate up to 1.0 mM; after that, an increase in concentration led to a decrease in degradation rates. At insufficient H_2O_2 doses, there is a decrease in the reaction due to the decrease in •OH generation, whilst an excess of H_2O_2 could lead to an increase in the scavenging effect of H_2O_2 on •OH radicals which can inhibit the reaction (Wang et al., 2016).

The line corresponding to a H_2O_2 concentration of 1.0 mM represents the degradation rate of methyl orange under the optimal operating conditions which follows: $[MO] = 10$ mg/L, catalyst loading = 2000 mg/L, $[H_2O_2] = 1.0$ mM, pH = 3 and UVB irradiation ($\lambda = 310$ nm – 350 nm). Under these optimal conditions, complete decolourisation of the methyl orange occurred 45 minutes after the reaction's activation upon the addition of H_2O_2. Upon the addition of H_2O_2, there was a steep increase in reaction rate, which after that decreased.

At insufficient H_2O_2 doses, there is a decrease in the reaction due to the decrease in •OH generation resulting from insufficient H_2O_2, whilst an excess of H_2O_2 could lead to an increase in the scavenging effect of H_2O_2 on •OH radicals which can inhibit the reaction (Wang et al., 2016). This can be seen in **Figure 14,** where an H_2O_2 concentration of 40 mM had a much

53

lower degradation rate than the optimal. The scavenging effect of excess H_2O_2 is shown by reaction 15 (Jiang et al., 2010):

$$H_2O_2 + \bullet OH \rightarrow H_2O + \bullet O_2H \qquad (15)$$

This new formed radical, hydroperoxyl radical ($\bullet O_2H$), has a lower redox potential (1.7 V) than the hydroxyl radical ($\bullet OH$), which has a redox potential of 2.7 V (Zhang et al., 2013, Wang and Wang, 2020). This also means that these radicals have a lower oxidising ability and thus can decrease the rate of degradation (Wang and Wang, 2020). With an H_2O_2 concentration of 1.0 mM, the complete decolourisation of methyl orange was achieved after 45 minutes of reaction time under complete optimal conditions.

6   CHAPTER SIX: DEGRADATION MECHANISM

6.1   Degradation Kinetics

Degradation kinetics were evaluated using methyl orange concentration data. The degradation of methyl orange (**Figure 15**) at different initial concentrations is directly dependent on the initial concentration, with a decrease in degradation rate with an increase in concentration. This difference is likely due to a variation in the stoichiometric ratio of the pollutant to H_2O_2, where the H_2O_2 is insufficient at higher concentrations. Other studies reported that the initial pollutant concentration had no effect on the rate of degradation of the system when a stoichiometric amount of H_2O_2 was added per the initial organic pollutant concentration (Rueda Marques et al., 2018).
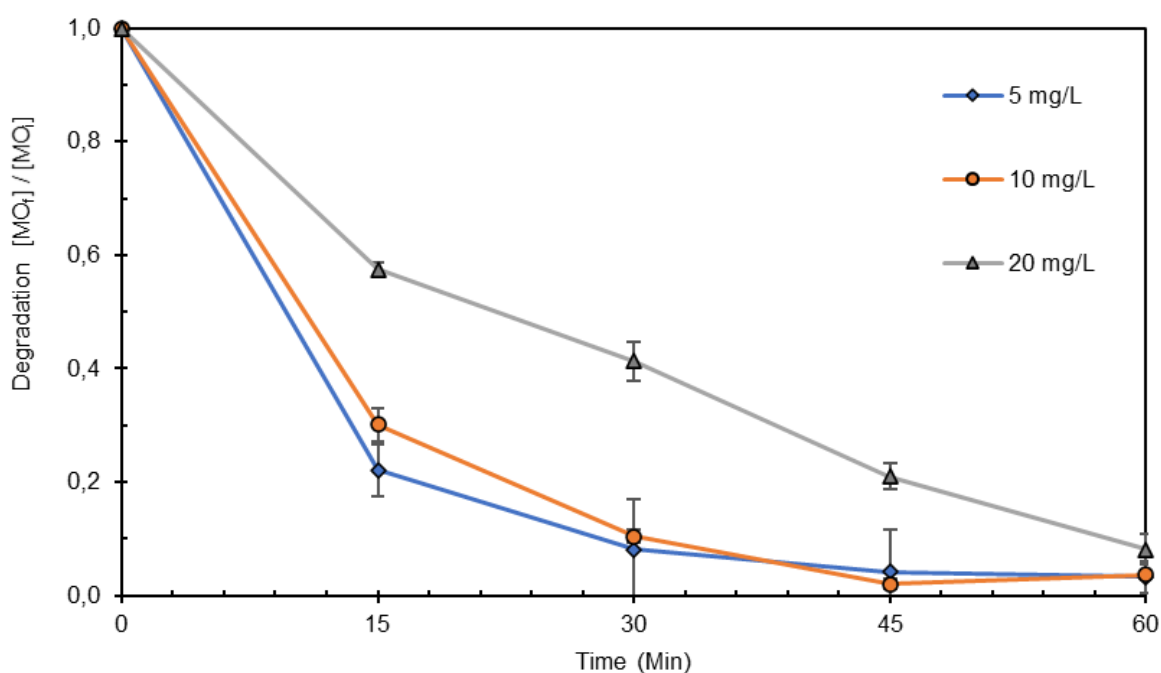
Figure 15:   The degradation of methyl orange over time at different initial concentrations. Operating conditions: [Ilmenite] = 2000 mg/L, [H_2O_2] = 1.0 mM, pH = 3, Irradiation = UVB (λ = 310 nm – 350 nm), Temperature = $\pm$ 20 °C

It is widely understood that the Fenton-like reaction mechanism is complex, consisting of several parallel reactions. This complexity makes conducting a detailed kinetic analysis

55

challenging, and therefore the data was fit to pseudo-first and pseudo-second-order models. The degradation kinetics of methyl orange using ilmenite as a catalyst in a Fenton-like process was fitted using the Langmuir-Hinshelwood model. The Langmuir-Hinshelwood model is used to explain a heterogeneous catalytic process (Kumar et al., 2008). The Langmuir-Hinshelwood equation is given below (equation 16):

$$r = \frac{dC}{dt} = \frac{k_r K C}{1 + K C'} \tag{16}$$

The equations for PFO and PSO were adjusted to their non-linearised forms (equations 17, 18) below (Zhang et al., 2017):

$$C = C_0 e^{-k_1 t} \tag{17}$$

$$C = \frac{C_0}{1 + k_2 t C_0} \tag{18}$$

Where C_0 is the initial concentration, k is the rate constant, and t is the time. The PFO and PSO modelling results for each concentration can be seen in **Figure 16** below.
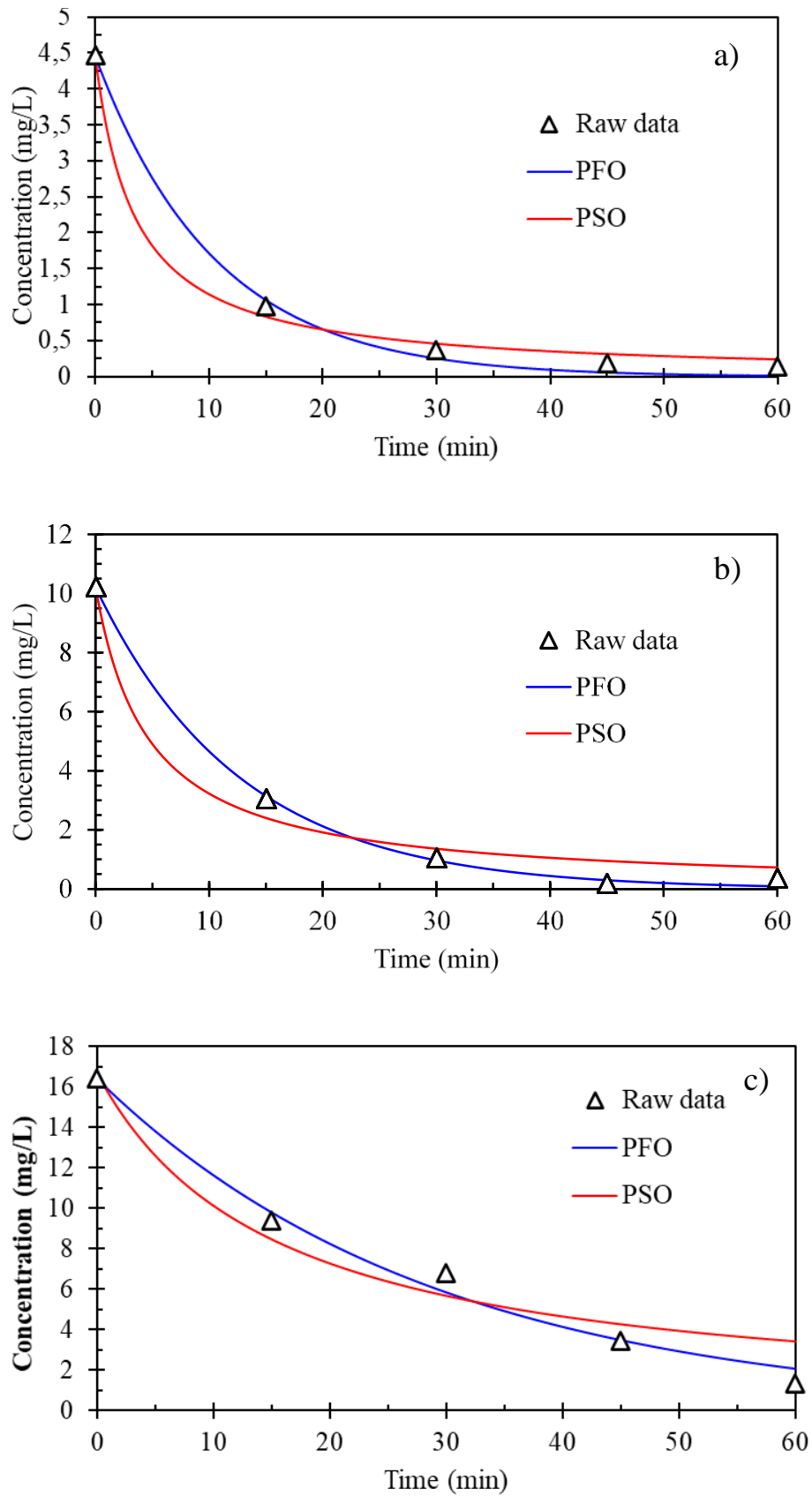
Figure 16: The PFO and PSO models of the Methyl Orange concentration data, a) 5 mg/L, b) 10 mg/L, c) 20 mg/L

57

The R^2 and k values for the PFO and PSO models are given in **Table 6**. Good fits were obtained for the PFO model with R^2 values of 0.996, 0.9985 and 0.9886 for 5 mg/L, 10 mg/L and 20 mg/L, respectively. Whilst the PSO model displayed R^2 values of 0.9957, 0.9828 and 0.9476 for the same concentrations. Although the PSO and PFO models fit the data for the 5 mg/L and 10 mg/L well, the PSO model does not fit the 20 mg/L data as precisely as the PFO model does.

Table 6: R^2 and k of the pseudo-first and pseudo-second-order modelling

Concentration	Pseudo-First-Order		Pseudo-Second-Order	
	κ (min^{-1})	R^2	κ (L/(mol.min^{-1})	R^2
5 mg/L	0.09538	0.996	0.06485	0.9957
10 mg/L	0.07856	0.9985	0.02120	0.9828
20 mg/L	0.03429	0.9886	0.003882	0.9476

These results indicate that the reaction follows a PFO reaction rate, but the PSO model can also provide a respectable accuracy level for predictions. It should be noted that the degradation kinetics of methyl orange in AOPs has resulted in some conflicting results, with some authors identifying the reaction as first-order (García-Muñoz et al., 2016b) and others as second-order (Youssef et al., 2016).

6.2   Methyl Orange Degradation

LC-MS was performed on samples of the solution to determine whether methyl orange was still detected following an hour of reaction time. A calibration curve was established for methyl orange from 0.1 μg/mL to 10 μg/mL; the curve can be seen in **Appendix B**.

Figure 17 shows the LC-MS results of the initial sample before the reaction activation. The sample was analysed for the presence of methyl orange. Methyl orange was detected as the compound present in the initial sample taken before the reaction activation. The methyl orange

58

compound had an m/z value of 304.08 and a retention time of 4.14 minutes. Methyl orange is commonly detected at around an m/z of 304 (Baiocchi et al., 2002, Dai et al., 2007).
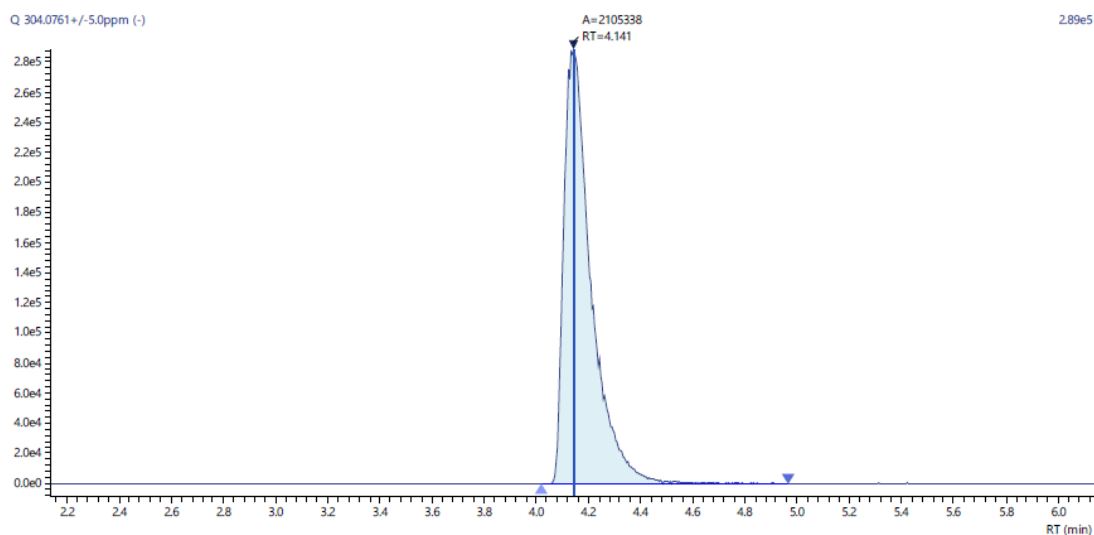
Figure 17:   Methyl Orange detected at T = 0 via LC-MS

A sample taken following 60 minutes of reaction time (T = 60) was analysed for methyl orange. The results are displayed graphically in **Figure 18**. It is evident that no methyl orange was detected in this sample, and therefore all methyl orange had been broken down by the reaction.

59
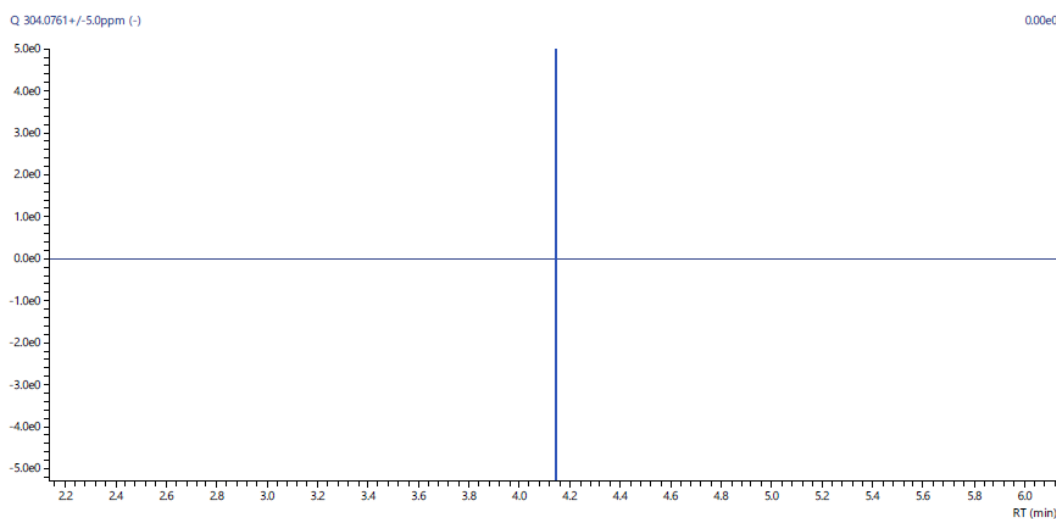
Figure 18:   Sample after the reaction at T = 60

This supports the results from the optimisation experiments where the colour visibly seen disappears and was confirmed by decreasing spectrophotometry values. These results prove that the reaction using ilmenite as a catalyst leading to at least the break down in the colour-creating bonds of the molecule. Methyl orange is an azo dye that creates the colour by an azo group or nitrogen-nitrogen double bond (N = N) (Hai, 2007, Schlichter et al., 2016).

6.3   Degree of Mineralisation

Following 60 minutes of reaction time, a 37 % TOC conversion was recorded. In order to determine whether a further decrease in TOC was obtainable, experiments were conducted in cycles with the stepwise addition of H_2O_2. It was speculated that there was a limiting factor in the reaction that had been fully utilised, either the catalyst or H_2O_2 dose. Due to the optimisation tests revealing that the excess catalyst loadings did not lead to an increase in reaction rate, it was assumed that H_2O_2 was the limiting factor. Some studies have shown that a stepwise addition of H_2O_2 can improve the efficiency of the Fenton process (Zhang et al., 2012).

Although it was speculated that H_2O_2 was the limiting reagent, it was also known that an excess of H_2O_2 could inhibit the reaction. It was decided that the H_2O_2 should be replenished after enough time had passed for it to have been depleted, thus avoiding the inhibiting effect of excess H_2O_2.

Experiments were conducted using optimal conditions with a 40 ml sample taken every 60 minutes, filtered and analysed for TOC. This experiment was repeated five times, 300 minutes in total, using the same solution. After the sample was taken at 60-minute intervals, a 1.0 mM dose of H_2O_2 was added to the solution. The volume of H_2O_2 was adjusted to account for the volume of solution remaining. These samples were analysed for TOC, and the results are displayed in **Figure 19**. The measured percentages of TOC can be seen in **Table 7,** with Time = 0 being the initial concentration of TOC detected.
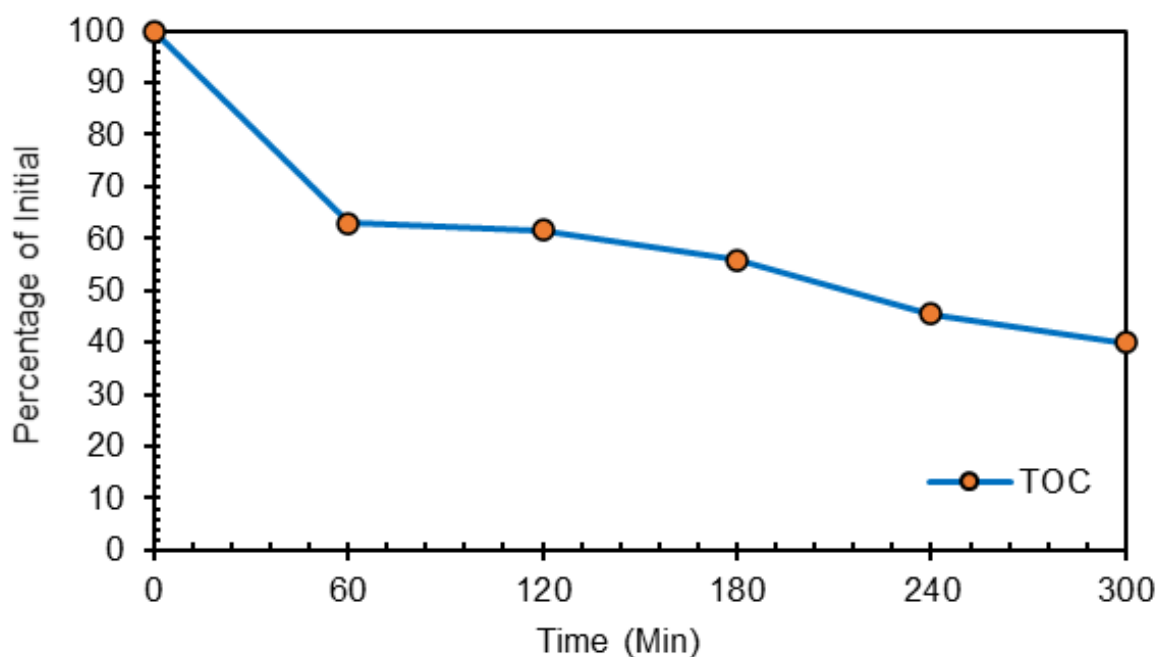

Figure 19:   The change in TOC (mg/L) over time with an addition of 1.0 mM H_2O_2 every 60 minutes. Operating conditions: [MO] = 10 mg/L, [H_2O_2] = 1.0 mM, [ilmenite] = 2000 mg/L, pH = 2.5, Irradiation = UVB (λ = 310 nm – 350 nm), temperature = ± 20 °C

Table 7:   The total percentage of TOC in solution, following five cycles, relative to the initial concentration detected.

Time	TOC (%)
0	100
60	62.95
120	61.59
180	55.95
240	45.46
300	39.99

TOC decrease from 100 % to 63 % following the first cycle. At the end of the five cycles, the TOC had decreased to 40 % of its original content, indicating a 60 % mineralisation. The most dramatic decrease in TOC was observed in the first 60 minutes. After that, the mineralisation rate slowed down, and only 20 % more TOC conversion was achieved in the last four cycles. A study conducted by García-Muñoz et al. (2016b) examined the effect of reduction pre-treatment on the catalytic activity of ilmenite. The study used TOC conversion of phenol as one of their parameters to observe catalytic stability. The study found that ilmenite had an initial stable activity but then a sudden deactivation. This was seen in the reduction of the treated ilmenite as well as the raw ilmenite. This is a potential explanation for the dramatic decrease in the rate of TOC conversion seen in **Figure 19**. García-Muñoz et al. (2016b) examined the reasoning for the deactivation and found that the iron oxidation states on the surface of the ilmenite catalyst had become oxidised.

In **Chapter 4**, it was through XRD analysis that the mineralogy of the catalyst had no significant changes following recovery from the Fenton-like process. Therefore the same conclusion as in the García-Muñoz et al. (2016b) seems likely, and the catalyst has become deactivated due to the oxidation of the iron on its surface. This further supports the idea in **Chapter 4** that the reaction initially occurs on the catalyst's surface and then takes place in the solution. The postulation is that the iron on the surface is reduced to Fe (II), the Fe (II) reacts with the H_2O_2 and is then oxidised back to Fe (III) on the surface.

6.4 Intermediates

The TOC and LC-MS analysis results reveal that although methyl orange is not present in the system following the reaction, there is still organic carbon content in the solution. This strongly indicates the formation of intermediates during the degradation process.

Many researchers have described the degradation pathway of Methyl Orange; however, most of these studies are performed using photocatalytic systems and not the Fenton process (Augugliaro et al., 2002, Baiocchi et al., 2002, Dai et al., 2007, Cohen et al., 2019).

Baiocchi et al. (2002) investigated the degradation pathway of methyl orange in a photocatalytic system using TiO_2. The following conditions were used: pH = 5.2, [MO] = 20 mg/L, Catalyst = 600 mg/L, Temperature = 55 °C, irradiation = $\leq$ 340 nm. The study made use of HPLC-MS analysis to determine the intermediates in the degradation of methyl orange. Samples were taken at various time intervals of 0, 5, 10, 15, 22 and 27 minutes of reaction time. Baiocchi et al. (2002) generated a fragmentation scheme of the main intermediates detected in the HPLC-MS analysis (**Figure 20**).
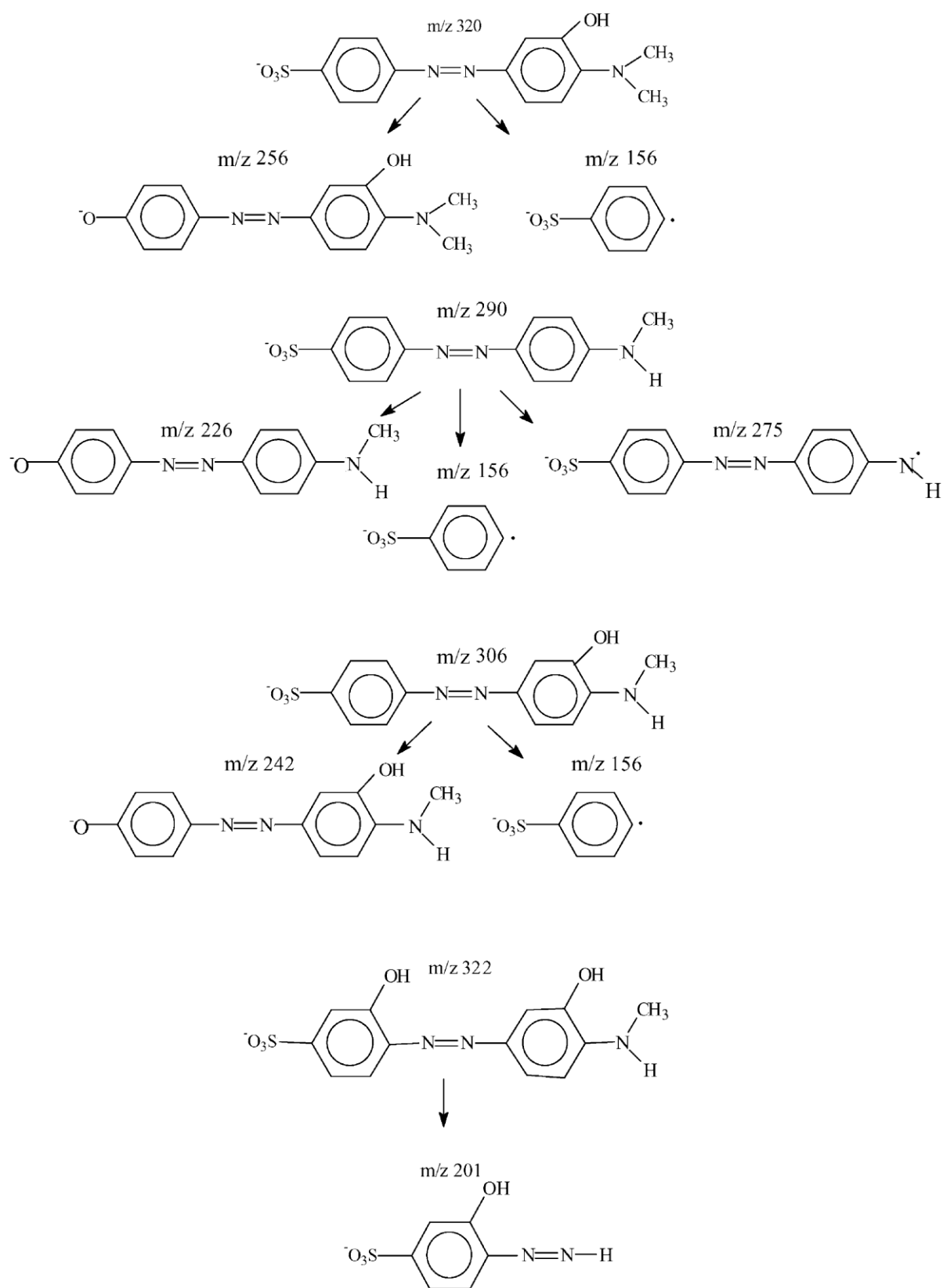
Figure 20: Methyl Orange fragmentation scheme by Baiocchi et al. (2002)

The study reported four intermediates with higher m/z values than the original compound, with only one exhibiting a long retention time. These are the formation of monohydroxylated and dehydroxylated products.

Dai et al. (2007) conducted a similar study using mesoporous titania nanoparticles as a photocatalyst for the degradation of methyl orange (pH = 2, m-TiO$_2$ = 1 g/L, MO = 20 ppm, Irradiation = UV). The study aimed to determine the intermediates formed before the decolourisation of the methyl orange, in other words, the intermediates that still contained the chromophoric group of azo dye bond (N=N). The authors analysed the intermediates using HPLC-MS and used this to infer the Methyl Orange degradation pathway. MS was used in the ESI ion source for the degradation of MO without UV irradiation. Analysis showed that methyl orange (m/z 304) fragments mainly into three molecules (m/z 289, m/z 240 and m/z 156) without irradiation. In the presence of UV irradiation, at least nine intermediates were detected. The analysis indicated the formation of intermediates with an introduced hydroxyl molecule on the methyl orange compound (D1; D2; D3; D4 & D5 on **Figure 21**).

On the other hand, Compound B experienced the loss of a methyl group. A compound E was also detected, which originated through the addition of a methyl group. **Figure 21** shows the different intermediates detected before the decolourisation of methyl orange.
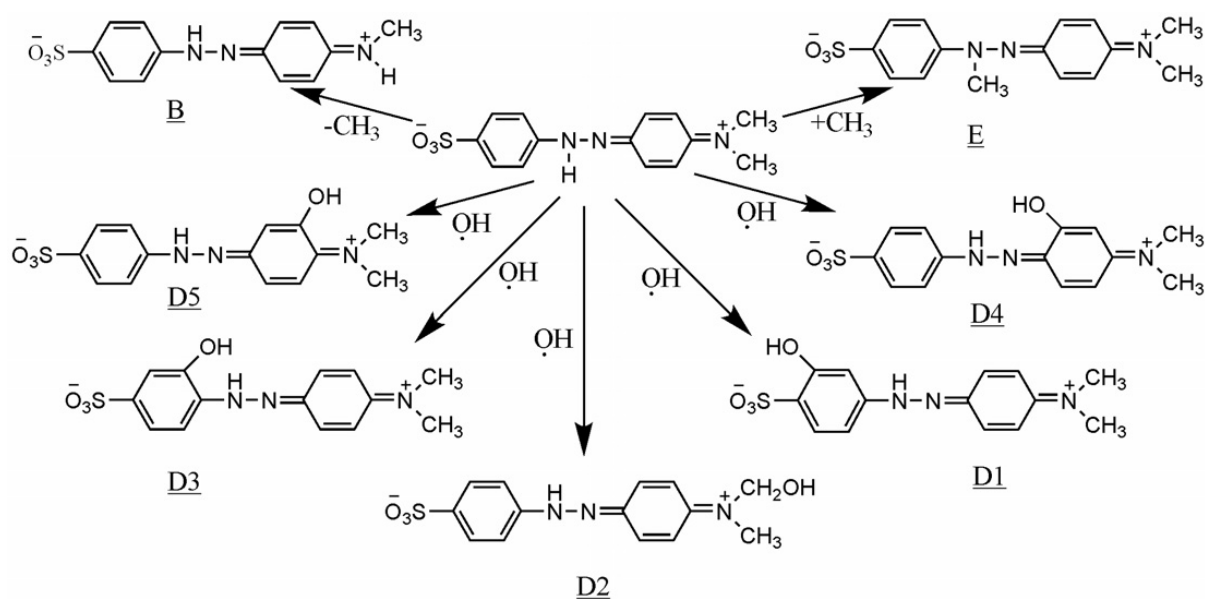
Figure 21: A Proposed photodegradation pathway of the quinonoid Methyl Orange by Dai et al. (2007)

65

The authors concluded that the formed intermediates were consistent with the degradation route of methyl orange through processes of demethylation, methylation and hydroxylation, with demethylation taking precedence over the others.

While it is helpful to understand the intermediates formed before the decolourisation of methyl orange, they are short-lived as the decolourisation process occurs quite rapidly. Therefore, these intermediates only provide an idea of the "starting compounds" before breaking the highly stable azo bond that makes these compounds so resistant to conventional degradation processes.

Cohen et al. (2019) conducted a study to investigate the degradation pathway of three organic contaminants, methyl orange, methylene blue and nitrophenol, in a Fenton process using synthesised maghemite (Υ-Fe_2O_3)/silica microspheres as a catalyst (Catalyst = 0.03 g/ml, H_2O_2 = 0.68 mol/L, pH = 3, Temperature = 40 °C. The degradation products were analysed using LC-MS and IC. Samples were taken at 2 min, 30 min, 60 min, 2h and 4h of reaction time. At a reaction time of 2 min, a peak at *m/z* 304 was detected, this value corresponds to the *m/z* of methyl orange, this peak was noted to disappear after 1 hour of reaction time, this was also noted in the present work whereby LC-MS detected no methyl orange after 1 hour of reaction time. Cohen et al. (2019) found that the degradation of methyl orange occurred through three mechanisms (**Figure 22**):

(1) The attack of •OH radicals on the benzene ring in the ortho-position resulted in the group's hydroxylation.
(2) The attack of •OH radicals in the benzene ring bonded to the azo group (C - N = N) cleaves the azo bond.
(3) The attack of •OH radicals at the methyl group of the amino function.
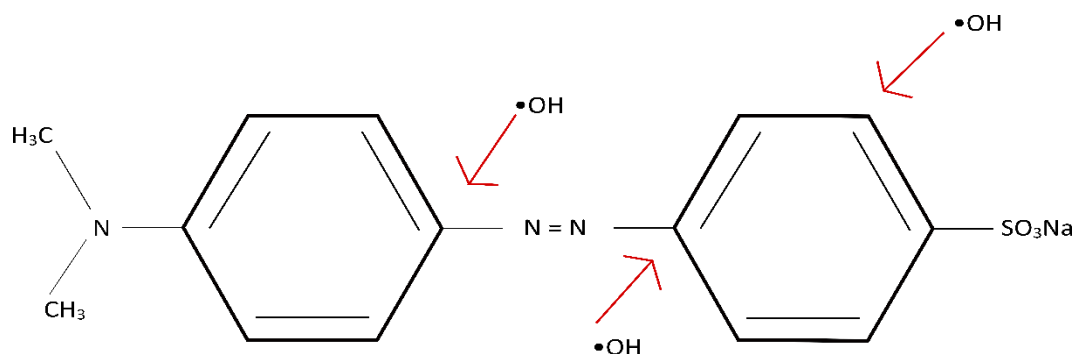
Figure 22: The mechanisms of •OH attack on methyl orange

66

The study found that reaction (1), hydroxylation, appears to be the primary degradation pathway. The study proposed a methyl orange degradation pathway that is displayed in **Figure 23**.
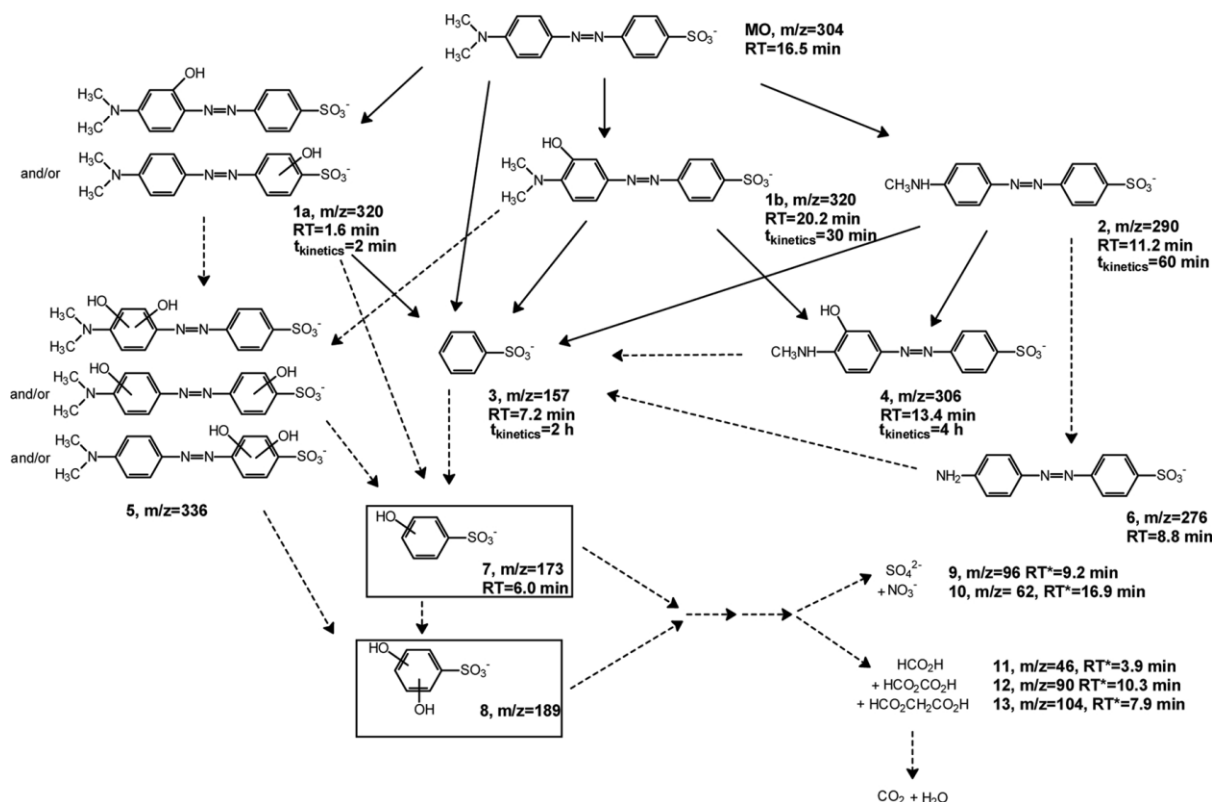
Figure 23: Proposed degradation pathway of methyl orange by Cohen et al. (2019)

The studies summarized above indicate similar degradation pathway mechanisms of methyl orange in different AOPs. In general, it appears that the methyl orange compound firstly undergoes hydroxylation, demethylation or methylation of the stem carbon chains attached to the benzene rings. This can lead to the generation of higher in weight (m/z) compounds than the original parent compound (Baiocchi et al., 2002). Furthermore, these compounds retain the azo bond (N=N), which gives the dye its colour (Dai et al., 2007). This is noted during the present study's experiments, whereby total decolourisation is only achieved after 45 minutes of reaction time under optimal operating conditions ([MO] = 10 m/L). Therefore, it is assumed that the intermediates formed within these 45 minutes structurally contain two benzene rings joined by an azo group. Intermediates tend to have *m/z* values ranging from 336 to 290 depending on whether the molecule underwent hydroxylation, methylation or demethylation.

Upon further oxidation of these methyl orange intermediates, the azo group undergoes cleavage of the N=N group splitting the molecule into two separate compounds containing a single

benzene ring. These compounds have lower m/z values ranging from 189 to 80 (Baiocchi et al., 2002, Cohen et al., 2019). These compounds detected by Cohen et al. (2019) were analogues of benzenesulfonate, one of which (m/z 156) was also detected by Baiocchi et al. (2002).

Lastly, the single benzene structured compounds undergo ring-opening reactions, leading to single-chain organic compounds and inorganic anions. Some of the compounds that have been detected at this stage are short-chain organic acids such as formic acid (H_2CO_2), Oxalic acid ($C_2H_2O_4$) and Malonic acid ($C_3H_4O_4$) (Cohen et al., 2019). Inorganic anions that have been found are mainly sulphates and nitrates. Of these compounds, Formic acid has low toxicity and is often used in many industrial processes (Wang and Bai, 2016). Malonic acid and oxalic acid have higher toxicity and thus are not necessarily considered safe.

In this work, total methyl orange degradation was achieved with a TOC conversion of approximately 60 %. Due to the complete loss of colour of the solution, it appears that the intermediates present after the reaction would likely to be either benzene-ring analogues or short-chain organic acids or both. Further research is required to determine the intermediates and assess the true extent of degradation of the compound.

7 CHAPTER SEVEN: PRACTICAL VIABILITY

7.1 Introduction

This study aimed to address some of the issues associated with the more conventionally used AOPs. The main issues being the high cost of implementation and the production of effluent with high levels of heavy metals due to leaching. This work aimed at addressing these issues whilst also maintaining the high efficiency of these AOPs at degrading highly stable compounds such as methyl orange. This chapter addresses the results obtained in the context of the issues mentioned and the practical viability of implementing this process in the real world.

7.2 Preliminary Cost Investigation

The total cost of implementing AOPs into real-world applications is difficult to assess accurately; however, a few aspects can be comparatively considered in the whole financial scheme:

- Cost of the materials
- Cost of implementation
- Cost of operation

The cost of materials refers to all the physical and chemical materials required to create the AOP system. This can include a range of items from catalysts and reagents to physical building materials and piping. The cost of implementation refers to the labour involved in creating these materials and constructing the system. The cost of operation considers the expense of maintenance and utility consumption (i.e., electricity). Most of these costs will vary greatly depending on plant design and regional area; therefore, an assessment will be made instead of materials needed to activate the AOP system. Expenses play a large role in the practical application of wastewater treatment processes. However, a full cost analysis is complex and thus only preliminary economic research was conducted.

69

7.2.1 Cost of Materials

The cost of materials is evaluated in terms of the materials needed to activate the AOP system, such as reagents and catalysts. The cost of ilmenite is compared directly to the cost of the commonly used catalyst titanium dioxide in **Table 8**. The costs were collected from Sigma Aldrich, a company the supplies materials to laboratories.

Table 8: The average cost of commonly used catalysts (sigmaaldrich.com)

Catalytic Material	Cost (R per gram)
Titanium Dioxide	3 114.50
Ilmenite	78.16

As can be seen above, the cost of ilmenite is far less than that of titanium dioxide, making it an attractive alternative for wastewater treatment.

7.3 Iron Leaching

One of the main issues addressed involving the Fenton process is the generation of heavy metal sludge. The use of a solid catalyst with minimal iron leaching is one of the ways to combat this issue. Water quality guidelines are set up to determine the maximum amount of iron in the water that can be used for different purposes.

7.3.1 South African Water Quality Guidelines

In 1996 the South African Department of Water Affairs and Forestry (DWAF, now known as the Department of Water and Sanitation (DWS)) published the first editions of the South African Water Quality Guidelines (SAWQG), comprising out of eight volumes. The eight volumes each deal with different water use purposes, from livestock watering and irrigation to domestic and recreation use of water. Amongst the most common water uses are domestic use, crop irrigation and industrial use. Therefore, these three types of water uses are investigated for potential water reuse purposes.

The definitions of each type of water use are taken from the SAWQGs and are as follows:

1. **Domestic use** refers to water used for drinking, food preparation, hygiene, washing, laundry and gardening (Department of Water Affairs and Forestry, CSIR Environmental Services, 1996c).

2. **Agricultural Irrigation use** refers to any water used for commercial crops, irrigation water supplies, garden watering and the production of floricultural crops and potted plants (Department of Water Affairs and Forestry, CSIR Environmental Services, 1996a).

3. **Industrial Use** refers to water used in industrial processes and includes water used for cooling, steam production, solvents, diluents and carriers. This category also includes water utilities such as fire protection and wash water (Department of Water Affairs and Forestry, CSIR Environmental Services, 1996d).

Standards are also set in place for aquatic ecosystems; this is because Section 21 (f) of the National Water Act (NWA) of South Africa allows for the discharging of water containing waste into a water resource (aquatic ecosystem) if permission is granted through a Water Use Licence. Aquatic ecosystems are defined as the abiotic and biotic components, habitats and ecological processes existing within natural water systems (E.g., rivers, wetlands) (Department of Water Affairs and Forestry, CSIR Environmental Services, 1996b). These guidelines are essential for the water quality that should be to be discharged into natural water sources. However, in 1999 the DWAF published two new sets of discharge limits and conditions, general limits and special limits (Department of Water Affairs and Forestry, 1999). The general and special limits for discharge into a natural water source is 0.3 mg/L.

Table 9 summarises the effects of iron in water for domestic, irrigation and industrial uses according to the SAWQGs.

Table 9: Concentration of Iron and its effects in different water uses according to the South African Water Quality Guidelines. Information is taken from (CSIR Environmental Services, 1996c, CSIR Environmental Services, 1996a, CSIR Environmental Services, 1996b, CSIR Environmental Services, 1996d)

Concentration of Iron (mg/L)	Effect		
	Domestic Use	**Agricultural Irrigation**	**Industrial Use**
0 – 0.1	**Health:** No health effects **Aesthetic:** No aesthetic effects	**Plant Toxicity:** These levels are not toxic to plant root uptake, but iron deposits can damage plant leaves when wetted by irrigation. **Irrigation Equipment:** Minor clogging problems	**Equipment:** No damage to equipment **Processes:** No Interference **Products:** No Effect **Waste Handling:** No problem
0.1 – 0.3	**Health:** No health effects **Aesthetic:** A slight effect on taste	**Plant Toxicity:** Same as above **Irrigation Equipment:** Moderate clogging problems	**Equipment:** Minor to moderate damage **Processes:** Minor Interference

			Products: Minor impairment **Waste Handling:** No problem
0.3 – 1.0	**Health:** No health effects **Aesthetic:** Adverse effect on taste	**Plant Toxicity:** Same as above **Irrigation Equipment:** Same as above	**Equipment:** Moderate to significant damage **Processes:** Moderate to significant interference **Products:** Moderate to significant impairment **Waste Handling:** No problem
1.0 - 10	**Health:** Slight health effects in children **Aesthetic:** Pronounced taste effect **Plumbing:**	**Plant Toxicity:** **5.0 – 20 mg/L** Maximum acceptable concentration for neutral and **alkaline soils.** **Irrigation Equipment:** **>1.5 mg/L**	**Equipment:** Significant to major damage **Processes:** Significant to major interference **Products:**

	Plumbing problems	Severe clogging problems	Significant to major impairment
			Waste Handling: Treatment required to precipitate excessive iron
10 – 30	**Health:** Chronic health effects in children	**Plant Toxicity:** **> 20 mg/L** It exceeds most guidelines and will impact the soil and plants.	
	Aesthetic: Severe taste effects		
	Plumbing: Severe plumbing effects	**Irrigation Equipment:** **>1.5 mg/L** Severe clogging problems	
30 - 100	**Health:** Long-term Health Effects		
	Aesthetic: Same as Above		
	Plumbing: Same as Above		
100 - 300	**Health:** Chronic Health Effects		
	Aesthetic: Same as Above		

	Plumbing:		
	Same as Above		
300 – 3000	Health:		
	Chronic and acute health effects.		
	Potential accidental poisoning.		
	Aesthetic:		
	Same as Above		
	Plumbing:		
	Same as Above		
3000 – 30 000	Health:		
	Lethal Toxicity		
	Aesthetic:		
	Same as Above		
	Plumbing:		
	Same as Above		

From **Table 9,** it is seen that adverse health effects of iron in drinking water start to occur at levels between 1.0 to 10 mg/L whilst negative impacts on equipment and industrial processes start above 0.3 mg/L. The highest level of measure iron in solution at optimal conditions was at 3.5 mg/L; at these levels, the water will not be suitable for industrial or agricultural reuse as it may cause problems with equipment. This level is, however, mainly safe for human consumption. This is further confirmed by the World Health Organisation (WHO) Guideline for Drinking Water Quality that states iron concentrations between 1.0 and 3.0 mg/L are acceptable for people drinking anaerobic well water (World Health Organization, 2008).

8 CHAPTER EIGHT: CONCLUSION AND RECOMMENDATIONS

8.1 Summary

Water reuse is one of the ways to keep up with the current water demand and remove harmful pollutants from wastewater to protect people's health and the environment. Most priority organic contaminants are resistant to conventional treatment technologies, and thus new and innovative ways of breaking down these harmful substances have become a widely researched topic. A very effective method of degrading these types of pollutants is through advanced oxidation processes. Most oxidative processes use catalysts to activate these intense reactions that lead to the degradation of these pollutants. However, many current catalysts lead to secondary issues, such as toxic sludge production, or are costly to implement. This study focused on using a naturally occurring titanium-iron oxide, ilmenite, as a catalyst in a Fenton-like process. The study aimed to determine whether the raw ilmenite could be used as an effective catalyst for the degradation of the highly stable azo dye methyl orange.

The catalyst was firstly characterised according to mineralogy, elemental composition and BET surface area. XRD analysis revealed that the catalyst consisted of 83 % ilmenite, 15 % hematite and 1.2 % rutile. This indicated that the material could work effectively in a Fenton-like process. The XRF analysis showed weight percentage contributions of 34.60 % Fe, 32.30 % Ti and 28.73 % O. These results are consistent with the data revealed by the XRD analysis. BET surface area was determined to be low at 10.42 m^2 which indicates an insufficient absorbance property.

Following catalyst characterisation, the Fenton-like process underwent optimisation to identify the optimal operating conditions in terms of pH and light, catalyst loading and H_2O_2 dose. The optimum operating conditions for a solution of 10 mg/L methyl orange were found to be 2000 mg/L of ilmenite, 1.0 mM H_2O_2, pH of 2.5 and UVB irradiation. Under these operating conditions, complete decolourisation was achieved following 45 minutes of reaction time. In conjunction with pH and catalyst loading optimisation, samples were collected to analyse the extent of iron leaching into the solution. Iron leaching quantities of approximately 3.5 mg/L were found under optimal operating conditions. This indicates that the reaction was primarily homogenous and occurred in solution.

Iron leaching does occur in the system but to a far lesser extent than what would occur in the classic Fenton's reaction. Although leaching does take place, this has a negligible impact on the mineralogy of the catalyst, which further supports the idea that the catalyst has high reusability. The degradation kinetics were modelled using the Langmuir-Hinshelwood model using experimental data, where the methyl orange concentration was changed using the optimal operating conditions. The modelling results showed that the kinetics best fit the PFO model for all three sets of experimental data but that the PSO also fit the data sets for 5 mg/L and 10 mg/L. Possible changes in kinetics and reaction behaviour can occur at larger quantities of the pollutant. However, this may be due to the insufficient amount of H_2O_2 stoichiometrically.

Analytical methodologies were employed to determine whether the target pollutant had undergone complete degradation and whether mineralisation had occurred. LC-MS results confirmed that after 60 minutes of reaction, no methyl orange was detected in the solution; this means the ilmenite in the Fenton-like process could degrade the dye completely. Total Organic Carbon analysis was conducted cyclically with stepwise additions of H_2O_2 every 60 minutes. TOC decreased the most dramatically within the first cycle to 62.92 %, thereafter TOC continued to decrease more gradually with a final TOC of 40 % following the five cycles. This indicates that the catalyst has reusability potential and that a looped system can be constructed to decrease TOC levels further. Complete TOC conversion was not achieved; therefore, the potential intermediates were hypothesised to be short chin organic acids, such as formic, oxalic and maleic acid and inorganic anions.

The study further assessed the practical viability of using this method in real-world applications. The mineral was found to be much more cost-effective compared to titanium dioxide. Iron leaching values were also compared with the South African Water Quality Guidelines in terms of different water use purposes and found that the concentration of iron in the water was close to the allowable limit for drinking water however would not be suitable for agricultural or industrial processes as it would cause plumbing issues.

8.2   Findings from the study

This study found that using ilmenite as a catalyst in a Photo-Fenton-Like reaction led to the complete decolourisation of methyl orange at optimal conditions following 45 minutes of reaction time. This work furthermore concluded that 60 % mineralisation had occurred.

Although this is only partial mineralisation, ilmenite effectively breaks down the highly complex and stable aromatic compounds. It is thought that the organic carbon remaining in the solution is possibly short-chain organic acids or phenolic type compounds. Such compounds are less stable than methyl orange and thus might be degraded using conventional biological treatment.

This work has shown that ilmenite can be used as a cost-effective naturally occurring catalyst for Fenton-like processes.

8.3   Recommendations for Future Work

Although this study has shown some of the potentials of naturally occurring minerals as catalysts for wastewater treatment, much more value can and should be done to contribute to this field of research. In particular a comparison between a variety of naturally occurring iron-bearing minerals, such as hematite, magnetite and goethite, would contribute to the knowledge of the influence of mineral structure and elemental composition of redox-active catalysts. Another aspect to consider when working with Fe-bearing catalysts is the potential of Fe ions in the system to inhibit full mineralisation through metal-ligand formation with short-chain organic acids, this should be included in future works.

In terms of ilmenite, investigations into the reaction mechanism that is involved in the process should continue. Intermediate compounds that remain in the solution should be analysed and identified.

It would also be worth investigating the potential of a two-phase system whereby wastewater treated using the ilmenite Fenton-like process can be passed through to a conventional biological type treatment such as activated sludge or a biofilm to determine whether the compounds are now suitable for this type of treatment.

In terms of practical viability, a full-scale cost analysis comparing different catalysts in different AOPs can provide beneficial information when evaluating wastewater treatment methods.

79

9   REFERENCES

Abdel-Raouf, N., Al-Homaidan, A. A. and Ibraheem, I. B. M. 2012. Microalgae and wastewater treatment. *Saudi Journal of Biological Sciences,* 19: pp. 257-275.

Al-Qaradawi, S. and Salman, S. R. 2002. Photocatalytic degradation of methyl orange as a model compound. *Journal of Photochemistry and Photobiology A: Chemistry,* 148: pp. 161-168.

Ameta, R., Chohadia, A. K., Jain, A. and Punjabi, P. B. 2018a. Fenton and Photo-Fenton Processes. *Advanced Oxidation Processes for Wastewater Treatment.*

Ameta, R., Solanki, M. S., Benjamin, S. and Ameta, S. C. 2018b. Photocatalysis. *Advanced Oxidation Processes for Wastewater Treatment.* Elsevier.

Ameta, S. C. and Ameta, R. 2018. Introduction. *In:* AMETA, S. C. & AMETA, R. (eds.) *Advanced Oxidation Processes for Wastewater Treatment: Emerging Green Chemical Technology.* 1 ed.: Academic Press.

Augugliaro, V., Baiocchi, C., Prevot, A. B., Garcia-Lopez, E., Loddo, V., Malato, S., Marci, G., Palmisano, L., Pazzi, M. and Pramauro, E. 2002. Azo-dyes photocatalytic degradation in aqueous suspension of TiO2 under solar irradiation. *Chemosphere,* 49: pp. 1223-1230.

Baiocchi, C., Brussino, M. C., Pramauro, E., Prevot, A. B., Palmisano, L. and Marci, G. 2002. Characterization of methyl orange and its photocatalytic degradation products by HPLC/UV– VIS diode array and atmospheric pressure ionization quadrupole ion trap mass spectrometry. *International Journal of Mass Spectrometry,* 214: pp. 247-256.

Bandara, J., Mielczarski, J. A. and Kiwi, J. 1999. 2. Photosensitized Degradation of Azo Dyes on Fe, Ti and Al Oxides. Mechanism of Charge Transfer during the Degradation. *Langmuir,* 15: pp. 7680-7687.

Barbusinski, K. 2009. Fenton Reacton - Controversy Concerning the Chemistry. *Ecological Chemistry and Engineering S,* 16 (3): pp. 347-358.

Beverskog, B. and Puigdomenech, I. 1996. Revised pourbaix diagrams for iron at 25-300oC. *Corrosion Science,* 38 (12): pp. 2121-2135.

Butt, A. L. and Tichapondwa 2020. Catalytic Wet Peroxide Oxidation of Methyl Orange using Naturally-Occurring South African Ilmenite as a Catalyst. *Chemical Engineering Transactions,* 81: pp. 367-371.

Canas-Martinez, D. M., Gauthier, G. H. and Pedraza-Avella, J. A. 2019. Photo-oxidative and photo-reductive capabilities of ilmenite-rich black sand concentrates using methyl orange as a probe molecule. *Photochemical & Photobiological Sciences,* (4).

Carbajo, J., García-Muñoz, P., Tolosana-Moranchel, A., Faraldos, M. and Bahamonde, A. 2014. Effect of water composition on the photocatalytic removal of pesticides with different TiO2 catalysts. *Environmental Science and Pollution Research,* 21: pp. 12233-12240.

Changotra, R., Rajput, H. and Dhir, A. 2017. Natural soil mediated photo fenton-like processes in treatment of pharmaceuticals: Batch and continuous approach. *Chemosphere,* 188: pp. 345-353.

Cohen, M., Ferroudj, N., Combes, A., Pichon, V. and Abramson, S. 2019. Tracking the degradation pathway of three model aqueous pollutants in a heterogeneous Fenton process. *Journal of Environmental Chemical Engineering,* 7.

Cornell, R. M. and Schwertmann, U. 2003. Solubility. *The Iron Oxides: Structure, Properties, Reactions, Occurences and Uses.* Weinheim, Germany: WILEY-VCH Verlag GmbH & Co. KGa A.

DEPARTMENT OF WATER AFFAIRS AND FORESTRY, 1996a. South African Water Quality Guidelines (Second Edition). Volume 4. CSIR Environmental Services

DEPARTMENT OF WATER AFFAIRS AND FORESTRY, 1996b. South African Water Quality Guidelines (Edition 1). Volume 7. CSIR Environmental Services

DEPARTMENT OF WATER AFFAIRS AND FORESTRY, 1996c. South African Water Quality Guidelines (Second Edition). Volume 1. CSIR Environmental Services

DEPARTMENT OF WATER AFFAIRS AND FORESTRY, 1996d. South African Water Quality Guidelines (Second Edition). Volume 3. CSIR Environmental Services

Dai, K., Chen, H., Peng, T., Ke, D. and Yi, H. 2007. Photocatalytic degradation of methyl orange in aqueous suspension of mesoporous titania nanoparticles. *Chemosphere,* 69: pp. 1361-1367.

Daneshvar, N., Salari, D. and Khataee, A. R. 2004. Photocatalytic degradation of azo dye acid red 14 in water on ZnO as an alternative catalyst to TiO2. *Journal of Photochemistry and Photobiology A: Chemistry,* 162: pp. 317-322.

1999. National Water Act Government Gazette No. 20526. Department of Water Affairs and Forestry

Devi, L. G., Kumar, S. G., Reddy, K. M. and Munikrishnappa, C. 2009. Photo degradation of Methyl Orange an azo dye by Advanced Fenton Process using zero valent metallic iron: Influence of various reaction parameters and its degradation mechanism. *Journal of Hazardous Material,* 164: pp. 459-467.

Domacena, A. M. G., Aquino, C. L. E. and Balela, M. D. L. 2020. Photo-Fenton Degradation of Methyl Orange Using Hematite (a-Fe2O3) of various morphologies. *Materials Today: Proceedings,* 22: pp. 248-254.

Eskandarian, M. R., Choi, H., Fazli, M. and Rasoulifard, M. H. 2016. Effect of UV-LED wavelength on direct photolytic and TiO2 photocatalytic degradation of emerging contaminants in water. *Chemical Engineering Journal,* 300: pp. 414-422.

Esteves, B. M., Rodrigues, C. S. D. and Madeira, L. M. 2019. Wastewater Treatment by Heterogeneous Fenton-Like Processes in Continuous Reactors. *In:* GIL, A., GALEANO, L. & VICENTE, M. (eds.) *Applications of Advanced Oxidation Processes (AOPs) to Drinking Water Treatment.* Springer International Publishing.

Fallmann, H., Krutzler, T., Bauer, R., Malato, S. and Blanco, J. 1999. Applicability of the Photo-Fenton method for treating water containing pesticides. *Catalysis Today*: pp. 309-319.

Fenton, H. J. H. 1894. Oxidation of tartaric acid in the presence of iron. *Journal of the Chemical Society, Transactions,* 65: pp. 899-911.

García-Muñoz, P., Pliego, G., Bahamonde, A. and Casas, J. A. 2017a. Sulfonamides photoassisted oxidation treatments catalyzed by ilmenite. *Chemosphere,* 180: pp. 523-530.

García-Muñoz, P., Pliego, G., Zazo, J. A., Bahamonde, A. and Casas, J. A. 2016a. Ilmenite (FeTiO3) as low cost catalyst for advanced oxidation processes. *Journal of Environmental Chemical Engineering,* 4: pp. 542-548.

García-Muñoz, P., Pliego, G., Zazo, J. A., Barbero, B., Bahamonde, A. and Casas, J. A. 2016b. Modified ilmenite as catalyst for CWPO-Photoassisted process under LED light. *Chemical Engineering Journal*.

García-Muñoz, P., Pliego, G., Zazo, J. A. and Casas, J. A. 2018. Photocatalytic wet peroxide oxidation process at circumneutral pH using ilmenite as catalyst. *Journal of Environmental Chemical Engineering,* 6: pp. 7312-7317.

García-Muñoz, P., Pliego, G., Zazo, J. A., Munoz, M., De Pedro, Z. M., Bahamonde, A. and Casas, J. A. 2017b. Treatment of hospital wastewater through the CWPO-Photoassisted process catalyzed by ilmenite. *Journal of Environmental Chemical Engineering,* 5: pp. 4337-4343.

Hadjltaief, H. B., Da Costa, P., Beaunier, P., Gálvez, M. E. and Zina, M. B. 2014. Fe-clay-plate as a heterogeneous catalyst in photo-Fenton oxidation of phenol as probe molecule for water treatment. *Applied Clay Science,* 91-92: pp. 46-54.

Hai, F. I. 2007. Hybrid Treatment Systems for Dye Wastewater. *Critical Reviews in Environmental Science and Technology,* 37 (4): pp. 315-377.

Hattori, Y. and Kaneko, K. 2013. Adsorption Properties. *Chemistry, Molecular Sciences and Chemical Engineering.* Second ed.: Elsevier.

Heggie, J. 2018. *Day Zero: Where next?* [Online]. National Geographic. Available: https://www.nationalgeographic.com/science/article/partner-content-south-africa-danger-of-running-out-of-water [Accessed].

Hofman-Caris, R. and Hofman, J. 2019. Limitations of Conventional Drinking Water Technologies in Pollutant Removal. *In:* GIL, A., GALEANO, L. & VICENTE, M. (eds.) *Applications of Advanced Oxidation Processes (AOPs) in Drinking Water Treatment.* Springer International Publishing.

Hopcroft, F. J. 2015. Wastewater Treament Processes. *Wastewater Treatment Concepts and Practices.* Momentum Press LLC.

Jafarinejad, S. 2017. Cost-Effective Catalytic Materials of AOP. *In:* GIL, A., GALEANO, L. & VICENTE, M. (eds.) *Applications of Advanced Oxidation Processes (AOPs) in Drinking Water Treatment.* Springer International Publishing AG 2017.

Jelic, A., Katsou, E., Malamis, S., Bolzonella, D. and Fatone, F. 2015. Occurrence, Removal, and Fate of PAHs and VOCs in Municipal Wastewater Treatment Plants: A Literature Review. *In:* FORSGREN, A. J. (ed.) *Wastewater Treatment: Occurrence and Fate of Polycyclic Aromatic Hydrocarbons (PAHs).* Sweden: CRC Press.

Jiang, C., Pang, S., Ouyang, F., Ma, J. and Jiang, J. 2010. A new insight into Fenton and Fenton-like processes for water treatment. *Journal of Hazardous Material,* 174: pp. 813-817.

Klein, C. and Dutrow, B. 2007. Crystal Chemistry and Systematic Descriptions of Oxides, Hydroxides, and Halides. *In:* O'CALLAGHAN, J. (ed.) *Mineral Science.*

Kordkandi, S. and Forouzesh, M. 2014. Application of full factorial design for methylene blue dye removal using heat-activated persulfate oxidation. *Journal of the Taiwan Institute of Chemical Engineers,* 45: pp. 2597-2604.

Kumar, K. V., Porkodi, K. and Rocha, F. 2008. Langmuir-Hinshelwood kinetics - A theoretical study. *Catalysis Communications,* 9: pp. 82-84.

Kuo, W. G. 1992. Decolorizing Dye Wastewater with Fenton's Reagent. *Water Research,* 26 (7): pp. 881-886.

Kurian, M. 2021. Advanced oxidation processes and nanomaterials -a review. *Cleaner Engineering and Technology,* 2.

Lu, A., Li, Y., Lv, M., Wang, C., Yang, L., Liu, J., Wang, Y. R., Wong, K. H. and Wong, P. K. 2007. Photocatalytic oxidation of methyl orange by natural V-bearing rutile under visible light. *Solar Energy Materials and Solar Cells,* 91: pp. 1849-1855.

Lu, M.-C., Chen, J.-N. and Huang, H.-H. 2002. Role of Goethite dissolution in the oxidation of 2-chlorophenol with hydrogen peroxide. *Chemosphere,* 46: pp. 131-136.

Lueder, U., Jorgensen, B. B., Kappler, A. and Schmidt, C. 2020. Photochemistry of iron in aquatic environments. *Environmental Science Processes & Impacts,* 22 (12): pp. 12-24.

Mak, C. H., Han, X., Du, M., Kai, J.-J., Tsang, K. F., Jia, G., Cheng, K.-C., Shen, H.-H. and Hsu, H.-Y. 2021. Heterogenization of homogeneous photocatalysts utilizing synthetic and natural support materials. *Journal of Materiald Chemistry A,* 9: pp. 4454-4504.

Minella, M., Marchetti, G., De Laurentiis, E., Malandrino, M., Maurino, V., Minero, C., Vione, D. and Hanna, K. 2014. Photo-Fenton oxidation of phenol with magnetite as iron source. *Applied Catalysis B: Environmental,* 154-155: pp. 102-109.

Munoz, M., De Pedro, Z. M., Casas, J. A. and Rodriguez, J. J. 2015. Preparation of magnetite-based catalysts and their application in heterogeneous Fenton oxidation – A review. *Applied Catalysis B: Environmental,* 176-177: pp. 249-265.

Munoz, M., Domínguez, P., De Pedro, Z. M. and Casas, J. A. 2017. Naturally-occurring iron minerals as inexpensive catalysts for CWPO. *Applied Catalysis B: Environmental,* 203: pp. 166-173.

AAYOG, N., 2019. National Institution for Transforming India, Ministry of Jal Shakti and Development, M. o. R.

Nidheesh, P. V. 2015. Heterogeneous Fenton catalysts for the abatement of organic pollutants from aqueous solution: a review. *Royal Society of Chemistry,* 5: pp. 40552 - 40577.

Oh, S.-Y., Kim, H.-W., Park, J.-M., Park, H.-S. and Yoon, C. 2009. Oxidation of polyvinyl alcohol by persulfate activated with heat, Fe2+, and zero-valent iron. *Journal of Hazardous Materials,* 168: pp. 346-351.

Oller, I., Malato, S. and Sanchez-Perez, J. A. 2011. Combination of Advanced Oxidation Processes and biological treatments for wastewater decontamination - A review. *Science of the Total Environment,* 409: pp. 4141-4166.

Ortiz, I., Rivero, M. J. and Margallo, M. 2019. Advanced oxidative and catakytic processes. *In:* GALANAKIS, C. & AGRAFIOTI, E. (eds.) *Sustainable Water and Wastewater Processing.* Netherlands: Elsivier.

Othman, A., Sultan, M., Becker, R., Alsefry, S., Alharbi, T., Gebremichael, E., Alharbi, H. and Abdelmohsen, K. 2018. Use of Geophysical and Remote Sensing Data for Assessment of Aquifer Depletion and Related Land Deformation. *Surveys in Geophysics,* 39: pp. 543-566.

Oturan, M. A. and Aaron, J.-J. 2014. Advanced Oxidation Processes in Water/Wastewater Treatment: Principles and Applications. A Review. *Critical Reviews in Environmental Science and Technology,* 44 (23): pp. 2577-2641.

Pataquiva-Mateus, A. Y., Zea, H. R. and Ramirez, J. H. 2017. Degradation of Orange II by Fenton reaction using ilmenite as catalyst. *Environmental Science and Pollution Research,* 24: pp. 6187-6194.

Pliego, G., García-Muñoz, P., Zazo, J. A., Casas, J. A. and Rodriguez, J. J. 2016. Improving the Fenton process by visible LED irradiation. *Environmental Science and Pollution Research,* 23: pp. 23449-23455.

Pliego, G., Zazo, J. A., García-Muñoz, P., Munoz, M., Casas, J. A. and Rodriguez, J. J. 2015. Trends in the Intensification of the Fenton Process for Wastewater Treatment: An Overview. *Critical Reviews in Environmental Science and Technology,* 45 (24): pp. 2611-2692.

Qasim, S. R. and Zhu, G. 2018a. Biological Waste Treatment. *Wastewater Treatment and Reuse: Theory and Design Examples.* CRC Press.

Qasim, S. R. and Zhu, G. 2018b. Grit Removal. *Wastewater Treatment and Reuse: Theory and Design Examples.* CRC Press

Taylor & Francis Group LLC.

Qasim, S. R. and Zhu, G. 2018c. Screening. *Wastewater Treatment and Reuse: Theory and Design Examples.* CRC Press

Taylor & Francis Group LLC.

Quadrado, R. F. N. and Fajardo, A. R. 2017. Fast decolorization of azo methyl orange via heterogeneous Fenton and Fenton-like reactions using alginate-Fe2+/Fe3+ films as catalysts. *Carbohydrate Polymers,* 177: pp. 443-450.

Riffat, R. 2013a. Primary treatment. *Fundamentals of wastewater treatment and engineering.*

Riffat, R. 2013b. Secondary treatment: Attached growth and combined processes. *Fundamentals of wastewater treatment and engineering.*

Riffat, R. 2013c. Secondary treatment: Suspended growth process. *Fundamentals of wastewater treatment and engineering.*

Riffat, R. 2013d. Wastewater treatment fundamentals. *Fundamentals of wastewater treatment and engineering.* CRC Press

IWA Publishing.

Rijkenberg, M. J. A., Fischer, A. C., Kroon, J. J., Gerringe, L. J. A., Timmermans, K. R., Wolterbeek, H. T. and de Baar, H. J. W. 2005. The influence of UV irradiation on the photoreduction of iron in the Southern Ocean. *Marine Chemistry,* 93: pp. 119-129.

Rijkenberg, M. J. A., Gerringe, L. J. A., Neale, P. J., Timmermans, K. R., Buma, A. G. J. and De Baar, H. J. W. 2004. UVA viability overrules UVB ozone depletion effects on the photoreduction of iron in the Southern Ocean. *Geophysical Research Letters,* 30: pp. 1-5.

Robinson, T., McMullan, G., Marchant, R. and Nigam, P. 2001. Remediation of dyes in textile effluent: a critical review on current treatment technologies with a proposed alternative. *Bioresource Technology,* 77: pp. 247-255.

Rueda Marques, J. J., Levchuk, I. and Sillanpaa, M. 2018. Application of catalytic wet peroxide oxidation for industrial and urban wastewater treatment: A review. *Catalysts,* 8 (12): pp. 673.

Sajjad, T. A. and Al-zobai, K. M. M. Investigation of the effect of intensity and direction of light on the removal of reactive blue dye from simulated wastewater using photo-Fenton oxidation under UV irradiation: Batch and continuous methods. 2nd International Scientific Conference of Al-Ayen University, 2020 Baghdad, Iraq. IOP Publishing.

Salgado, P., Melin, V., Contreras, D., Moreno, Y. and Mansilla, H. 2013. Fenton Reaction Driven by Iron Ligands. *Journal of the Chilean Chemical Society,* 58 (4): pp. 2096-2101.

Schlichter, S., Diez, A. S., Zenobi, M. C., Dennehy, M. and Alvarez, M. 2016. Multi-Metal-Substituted-Goethite as an Effective Catalyst for Azo Dye Wastewater Oxidation. *Clean - Soil, Air, Water,* 44 (12): pp. 1652-1660.

Silva, E. N., Brasileiro, I. L. O., Madeira, V. S., de Farias, B. A., Ramalho, M. L. A., Rodriguez-Aguado, E. and Rodrigues-Castellon, E. 2020. Reusable CuFe2O4-Fe2O3 catalyst synthesis and application for the heterogenous photo-Fenton degradation of methylene blue in visible light. *Journal of Environmental Chemical Engineering,* 8.

Silveira, J. E., Claro, E. M. T., Paz, W. S., Oliveira, A. S., Zazo, J. A. and Casas, J. A. 2018. Optimization of Disperse Blue 3 mineralization by UV-LED/FeTiO 3 activated persulfate using response surface methodology. *Journal of the Taiwan Institute of Chemical Engineers,* 85: pp. 66-73.

Silveira, J. E., Paz, W. S., García-Muñoz, P., Zazo, J. A. and Casas, J. A. 2017. UV-LED/ilmenite/persulfate for azo dye mineralization: The role ofsulfate in the catalyst deactivation. *Applied Catalysis B: Environmental,* 219: pp. 314-321.

Soon, A. N. and JHameed, B. H. 2011. Heterogeneous catalytic treatment of synthetic dyes in aqueous media using Fenton and photo-assisted Fenton process. *Desalination,* 269: pp. 1-16.

Sparks, D. L. 2003a. Chemistry of Soil Organic Matter. *In:* CRUMLY, C. R. (ed.) *Environmental Soil Chemistry.* 2nd ed. USA: Elsevier Science (USA).

Sparks, D. L. 2003b. *Environmental Soil Chemistry*, Academic Press.

Teel, A. L., Ahmad, M. and Watts, R. J. 2011. Persulfate activation by naturally occuring trace minerals. *Journal of Hazardous Materials,* 196: pp. 153-159.

Tehrani-Bagha, A. R. and Balchi, T. 2018. Catalytic Wet Peroxide Oxidation. *In:* AMETA, R. & AMETA, S. C. (eds.) *Advanced Oxidation Processes for Wastewater Treament.* Elsevier.

Tichapondwa, S. M., Newman, J. P. and Kubheka, O. 2020. Effect of TiO2 phase on the photocatalytic degradation of methylene blue dye. *Physics and Chemistry of the Earth,* 118-119 (2020): pp. 1-6.

Tokumura, M., Morito, R., Hatayama, R. and Kawase, Y. 2011. Iron redox cycling in hydroxyl radical generation during the photo-Fenton oxidative degradation: Dynamic change of hydroxyl radical concentration. *Applied Catalysis B: Environmental,* 106: pp. 565-576.

Valhondo, C. and Carrera, J. 2019. Water as a finite resource: From historical accomplishments to emerging challenges and artificial recharge. *In:* GALANAKIS, C. & AGRAFIOTI, E. (eds.) *Sustainable Water and Wastewater Processing.* Netherlands: Elsevier.

Walker, C. H. 2009. Polycyclic Aromatic Hydrocarbons. *Organic Pollutants: An Ecotoxicological Perspective.* Second ed.: CRC Press.

Walling, C. 1975. Fenton's Reagent Revisited. *Accounts of Chemical Research,* 8: pp. 125-131.

Wang, J. and Bai, R. 2016. Formic acid enhanced effective degradation of methyl orange dye in aqueous solutions under UV-Vis irradiation. *Water Research,* 101: pp. 103-113.

Wang, J. and Wang, S. 2020. Reactive species in advanced oxidation processes: Formation, identification and reaction mechanism. *Chemical Engineering Journal,* 401: pp. 1-19.

Wang, N., Zheng, T., Zhang, G. and Wang, P. 2016. A review on Fenton-like processes for organic wastewater treatment. *Journal of Environmental Chemical Engineering,* 4: pp. 762-787.

Wang, Y. R. and Chu, W. 2012. Photo-assisted degradation of 2,4,5-trichlorophenoxyacetic acid by Fe(II)-catalyzed activation of Oxone process: The role of UV irradiation, reaction mechanism and mineralization. *Applied Catalysis B: Environmental,* 123-124: pp. 151-161.

Water Research Commission 2014. Parched prospects: The Emerging Water Crisis in South Africa. *Water Wheel,* 13 (6): pp. 42-47.

World Health Organization 2008. Guideline for Drinking-water Quality. 3 ed. Geneva, Switzerland: World Health Organization.

Xu, X. and Li, X.-Z. 2010. Degradation of azo dye Orange G in aqueous solutions by persulfate with ferrous ion. *Separation and Purification Technology,* 72: pp. 105-111.

Youssef, N. A., Shaban, S. A., Ibrahim, F. A. and Mahmoud, A. S. 2016. Degradation of methyl orange using Fenton catalytic reaction. *Egyptian Journal of Petroleum,* 25: pp. 317-321.

Yurdakal, S., Garlisi, C., Ozcan, L., Bellardita, M. and Palmisano, G. 2019. (Photo)catalyst Characterisation Techniques: Adsorption Isotherms and BET, SEM, FTIR, UV-VIS, Photoluminescence and Electrochemical Characteriszations. *In:* MARCI, G. & PALMISANO, L. (eds.) *Heterogeneous Photocatalysis: Relationships with Heterogeneous Catalysis and Perspectives.* Elsevier.

Zhang, H., Liu, D., Ren, S. and Zhang, H. 2017. Kinetic studies of direct blue photodegradation over flower-like TiO2. *Research on Chemical Intermediates,* 43: pp. 1529-1542.

Zhang, H., Wu, X. and Li, X. 2012. Oxidation and coagulation removal of COD from landfil leachate by Fered-Fenton process. *Chemical Engineering Journal,* 210: pp. 188-194.

Zhang, T., Zhu, H. and Croue, J.-P. 2013. Production of Sulfate Radical from Peroxymonosulfate Induced by a Magnetically Separable CuFe2O4 Spinel in Water: Efficiency, Stability, and Mechanism. *Environmental Science and Technology,* 47: pp. 2784-2781.

APPENDICES

Appendix A: XRF Report

CLIENT:	Alicia Butt			
PO NUMBER:	t.b.c.			
DATE:	2019-03-12			
ANALYSIS:	XRF			

ANALYSIS: The samples were prepared as pressed powders. 10-30g powdered sample, mixed with 20 drops Moviol (PVA), pressed to 10 tons.

The Thermo Fisher ARL Perform'X Sequential XRF instrument with Uniquant software was used for analyses.

The software analyse for all elements in the periodic table between Na and U, but only elements found

above the detection limits were reported.

The values were normalised, as no LOI was done to determine crystal water and oxidation state changes.

A standard sample material was prepared and analysed in the same manner as the samples and is reported as such.

Internal office use sample numbering: 1

	STANDARD		
	SARM 59 Ilmenite	**SARM 59 Analysed**	**ILMENITE**
SiO2	0,75	1,09	2,87
Al2O3	0,61	1,03	1,18
MgO	0,56	0,71	1,20
Na2O	-	0,22	0,25
P2O5	-	0,03	0,05
Fe2O3	50,3	48,27	49,47
K2O	-	0,03	0,05
CaO	0,05	0,07	0,24
TiO2	48,8	46,76	43,09
V2O5	0,25	0,42	0,39
Cr2O3	0,1	0,10	0,11
MnO	1,05	1,09	1,23
NiO	-	0,01	0,01
CuO	-		0,01
ZrO2	-	0,10	
TOTAL		99,93	100,16

If you have any further queries, kindly contact the laboratory.

Analyst: **J.E. Dykstra**
XRF Analyst

Figure 24: XRF Report of the raw catalyst sample
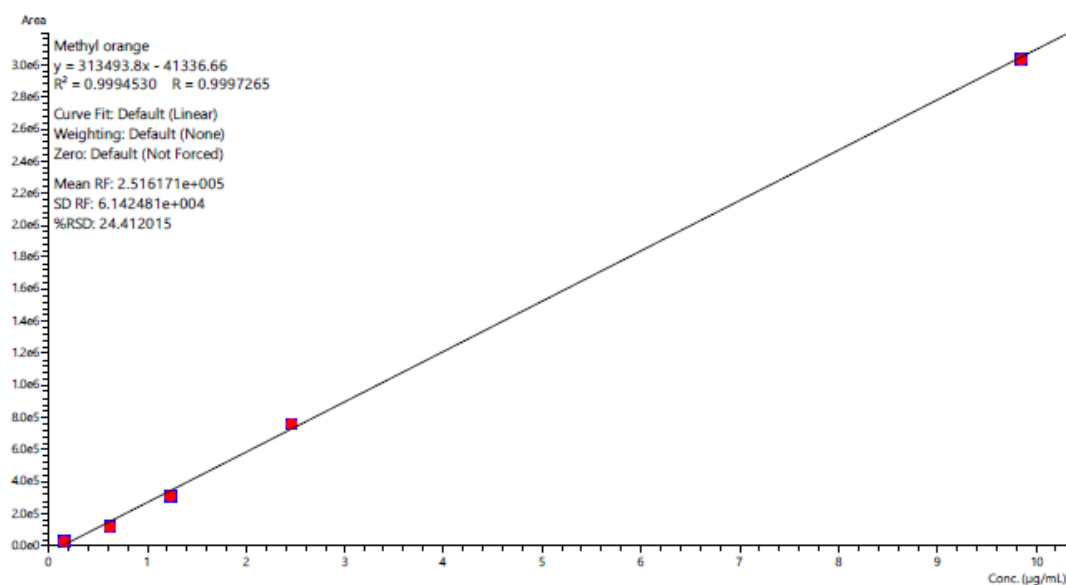
Appendix B: XRF Report

Figure 25:   Calibration curve for Methyl Orange (0.1 μg/mL to 10 μg/mL)

The calibration follows a linear function with the equation y = 313493.8x – 41336.66 and an R^2-value of 0.999.